M 2022

U.PORTO
FEUP FACULDADE DE ENGENHARIA
UNIVERSIDADE DO PORTO

Dip Content Study on Textile Reinforcements for Rubberized Applications

CRISTIANA ALEXANDRA NUNES PEREIRA

DISSERTAÇÃO DE MESTRADO APRESENTADA
À FACULDADE DE ENGENHARIA DA UNIVERSIDADE DO PORTO EM
ENGENHARIA QUÍMICA

Master in Chemical Engineering

Dip Content Study on Textile Reinforcements for Rubberized Applications

A Master's dissertation

of

Cristiana Alexandra Nunes Pereira

Developed within the course of the dissertation

held in

Continental – Indústria Têxtil do Ave, S. A.

Supervisor at FEUP: **Prof. Joana Peres**

Co-supervisor at FEUP: **Prof. Margarida Bastos**

Coordinator at C-ITA: **Eng. Ana Martins**

August 2022

Acknowledgment

I would like to thank to PI Department team, Eng. Carla Pires, Eng. Raul Falcão, Eng. Pedro Costa and Eng. Magda Dias for all the help when I needed and for the good ambiance. A special thanks to my coordinator, Eng. Ana Martins, for all support and guidance throughout the whole project.

To my lab co-workers, specially Rúben, Joaquim, Rui and Pedro for the availability to help in any situation and good work environment.

To Professor Joana Peres and Professor Margarida Bastos, for all the dedication to my work, and for tireless effort in helping me with all my doubts.

To my colleagues in this adventure, Maria and Inês, I thank you for all the great moments and for all the help during these months, I wish you the best.

To my friends, especially my beautiful “fishmongers”, for all the unforgettable moments and for making college such a beautiful and crazy journey.

A special thanks to the most important people of my life, my mother Elisabete, my dad Armando and my sister Filomena. Thank you for all you have done for me, thank you for all your hard work and for not letting me give up in any circumstance.

Professor Joana Peres and Margarida Bastos, supervisor and co-supervisior of this dissertation, are integrated members of LEPABE – Laboratory for Process Engineering, Environment, Biotechnology and Energy, financially supported by LA/P/0045/2020 (ALiCE), UIDB/00511/2020 and UIDP/00511/2020 (LEPABE), funded by national funds through FCT/MCTES (PIDDAC).

FCT Fundação para a Ciência e a Tecnologia
MINISTÉRIO DA CIÊNCIA, TECNOLOGIA E ENSINO SUPERIOR

REPÚBLICA PORTUGUESA

Abstract

Tires are the essential point of contact between the road and the vehicle, where their structure and behavior are much more complex than they appear to be. Tire textile reinforcements are crucial for a good performance of a tire, and their production involves a physical and chemical treatment using a dipping solution for their coating, conferring the capability of adhesion between cords and rubber composites. To have proper quality control of this treatment, it is necessary to quantify the amount of dip in cords. Currently, in Continental-Indústria Têxtil do Ave, S.A. (C-ITA), three different methods can be performed for determining this property: Wet-Chemical Method, Weighing Method, and Time Domain-Nuclear Magnetic Resonance (TD-NMR) analysis.

The main goal of this project was to calibrate the TD-NMR device for Rayon treated with Cokoon dipping solution since the TD-NMR analysis allows C-ITA to achieve faster quantification tests of the dip on the fiber and no need to resort to hazardous chemicals associated with Wet-Chemical Method. However, since the Cokoon dipping solution was recently developed, it was necessary to study the standard Wet-Chemical Method used for quantifying the dip content in Rayon cords. A comparison of different methods was made, and the results prove that the Wet-Chemical Method cannot be used for the new dipping solution. The Weighing Method was suggested as an alternative technique to the Wet-Chemical Method for Cokoon Dipped Rayon since it is non-destructive and does not interfere with the dipping solution. Thus, the calibration curve for Cokoon dipped Rayon was successfully made using the Weighing Method as a reference; however, to validate the curve, a correlation between the Wet-Chemical Method and the Weighing Method was made to be possible to obtain the dip content in the cord corresponding to the Weighing Method without performing this one. The validation of the curve was performed with 20 samples, but only three of them met the criterion established for the measurement's values by the two methods: TD-NMR and the Weighing Method. However, just two of the samples used have an acceptable time of storage, being the others from 2020 and 2021. So, these samples supported an investigation concerning Rayon mechanical properties' influence in TD-NMR analysis. The results obtained from the Bending Stiffness test induced that the increase in storage time of samples, increases the stiffness of the samples and decreases the quantity of dipping solution measured in the TD-NMR.

Keywords (theme): Tire; Rayon; TD-NMR; Dipping solution; Fibers;

Resumo

Os pneus são o ponto essencial de contacto entre a estrada e o veículo, sendo a sua estrutura e comportamento muito mais complexos do que aparentam ser. Os reforços têxteis dos pneus são cruciais para um bom desempenho de um pneu e a sua preparação envolve um tratamento físico e químico utilizando uma solução de impregnação para o seu revestimento, conferindo a capacidade de adesão entre as cordas e os compósitos de borracha. Para ter um controlo de qualidade adequado deste tratamento, é necessário quantificar o teor de sólidos impregnados nas cordas. Atualmente, na Continental-Indústria Têxtil do Ave, S.A. (C-ITA), podem ser utilizados três métodos diferentes para determinar esta propriedade: Método Químico, Método de Pesagem, e Análise por Ressonância Magnética Nuclear no Domínio do Tempo (TD-NMR).

O principal objetivo deste projeto foi calibrar o equipamento TD-NMR para o Rayon impregnado com a solução de impregnação Cokoon, uma vez que a análise TD-NMR permite à C-ITA alcançar testes de quantificação do conteúdo impregnado nas cordas mais rápidos e sem necessidade de recorrer a produtos químicos perigosos, associados ao Método Químico. Contudo, uma vez que a solução de impregnação Cokoon foi recentemente desenvolvida, foi necessário estudar o método convencional, Método Químico, utilizado para quantificar o teor de sólidos impregnado em cordas de Rayon. Foi feita uma comparação de diferentes métodos e os resultados provam que o Método Químico não pode ser utilizado para a solução de impregnação Cokoon. O Método de Pesagem foi sugerido como uma técnica alternativa ao Método Químico para Rayon impregnado com Cokoon, uma vez que é um método não destrutivo e não envolve interferência com a solução de impregnação. Assim, a curva de calibração para o Rayon impregnado com Cokoon foi realizada com sucesso utilizando o Método de Pesagem como referência; contudo, para validar a curva, foi realizada uma correlação entre o Método Químico e o Método de Pesagem, de forma a ser possível obter uma quantidade de soluto de impregnação nas cordas correspondente ao Método de Pesagem sem executar este método. A validação da curva foi desenvolvida com 20 amostras mas apenas três delas cumpriram o critério estabelecido para a diferença de valores medidos pelos dois métodos: TD-NMR e o Método de Pesagem. Contudo, apenas duas das amostras utilizadas tinham um tempo de armazenamento aceitável (inferior a 6 meses), sendo as restantes de 2020 e 2021. Assim, estas amostras serviram para suportar uma investigação relativa à influência das propriedades mecânicas do Rayon na análise realizada no TD-NMR. Os resultados obtidos a partir do teste de rigidez à flexão indiciam que com o aumento do tempo de armazenamento das amostras aumenta a rigidez destas e diminui a quantidade de solução de impregnação medida no TD-NMR.

Palavras-chave: Pneu; Rayon; TD-NMR; Solução de impregnação; Fibras;

Declaration

I hereby declare, under word of honor, that this work is original and that all non-original contributions were properly referenced with source identification.

Porto, 1 of August of 2022

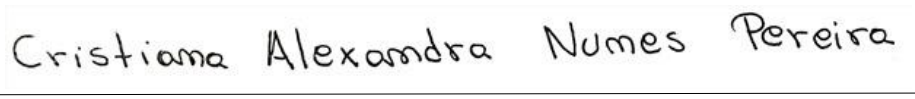

(Cristiana Alexandra Nunes Pereira)

Index

List of Figures

List of Tables

Notation and Glossary

dtex	decitex	g/ 10000 m
$\mathrm{DPU}_{\mathrm{per\ dipped\ cord}}$	Dip Pick-up per dipped cord	%
$\mathrm{DPU}_{\mathrm{per\ greige\ cord}}$	Dip Pick-up per greige cord	%
m_{dip}	mass of dipping solution	g
$m_{\mathrm{dipped\ cord}}$	mass of dipped cord	g
$m_{\mathrm{greige\ cord}}$	mass of greige cord	g
n	principal quantum number	
R^2	Determination coefficient	%
SE	Standard Error	
SC	Solid Content	%
SD	Standard Deviation	

Greek Letters

α	Significance Level
μ	Mean of a population
σ^2	Variance of a population

List of Acronyms

CI	Confidence Interval
C-ITA	Continental – Indústria Têxtil do Ave, S.A
DPU	Dip Pick-up
FID	Free Induction Decay
ITA	Indústria Têxtil do Ave
KCM	Kordsa-Chemical Method
LDU	Lab Dipping Unit
LTL	Lower Target Limit
PD	Production Department
PDU	Production Dipping Unit
PET	Polyethylene Terephthalate
RFL	Resorcinol-Formaldehyde-Latex
T	Target
TD-NMR	Time-Domain Nuclear Magnetic Resonance
UTL	Upper Target Limit
WCM	Wet-Chemical Method
WM	Weighing Method

1 Introduction

The road vehicle's operational properties result from the dynamic interaction of several components of the vehicle structure, and tires are the key components (Lugner, 2019).

Tire technology is a complex combination of science and engineering. Thus, knowledge in different fields is required to develop a tire, making its structure and behavior much more complex than they appear to be (Burak Erman, 2013).

The automotive industry's competitiveness and continuous market growth have forced tire companies to apply new and innovative technologies over the last 100 years to improve tire manufacturing and turn them into top-quality tires. Several branches of industry play an essential role in the manufacture of tires (Figure 1). These industries supply the raw materials required to achieve products with an ideal performance that satisfy the customer needs (Continental, 2022a).

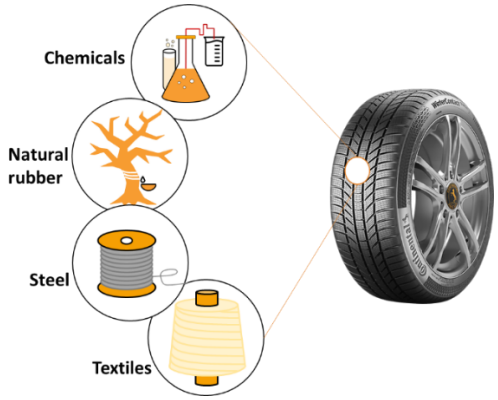

Figure 1. Main industries involved in tire manufacture. Adapted from (Continental, 2015b).

The textile industry supplies basic materials to produce cords or fabrics that serve to reinforce the tires. These reinforcements are a crucial part of tires since they work as the tire's skeleton, maintaining the air pressure inside the tire and providing sidewall stability, requirements needed by quality tires.

1.1 Company's Presentation

Indústria Têxtil do Ave, ITA, was founded in 1950 in Lousado, Portugal, starting with cotton canvas production. Over the years, cotton was replaced by raw materials such as rayon, nylon, polyester, and aramid with the purpose of producing textile reinforcements for Mabor tires. Between 1990 and 1993, Continental took complete control of the Portuguese companies, Mabor for tire production, and ITA to produce textile cords for the rubber industry. In this way, ITA changed its name to Continental – Indústria Têxtil do AVE and since then has continued to

grow so that today, in addition to being a supplier of textile reinforcements, it is also a company centered on textile development and investigation (Continental).

Continental is a recognized multinational, among the world's top 5 automotive suppliers contributing to safer driving and global environmental protection. It was founded in 1871 in Hannover, Germany, and the central business idea was the production of rubberized fabrics and solid tires for carriages and bicycles. Over the years, this company's continuous evolution was noted, allowing it to expand into more areas. Currently, Continental has approximately 193,000 employees in 58 countries working in the following areas: Chassis & Safety, Powertrain, Interior, ContiTech, and Tires (Continental, 2015a).

1.2 Framing and presentation of the work

The production process of textile reinforcements for tires in C-ITA is generically represented in Figure 2.

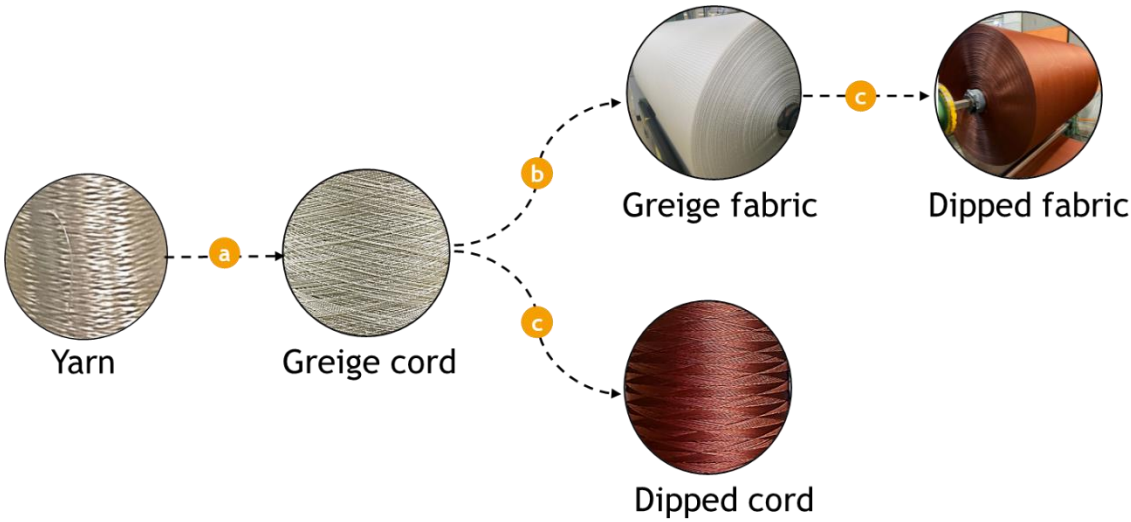

Figure 2. Production of textiles reinforcements. (a) - twisting, (b) - weaving, (c) - dipping.

The production of textile reinforcements for a tire comprises the production of dipped cords (Figure 2 (a-c) and dipped fabrics (Figure 2 (a-b-c)). Dipped cords require two steps: a twisting process (Figure 2 (a)) of the yarns to obtain greige cords and then a dipping process (Figure 2 (c)). In fabrics, an intermediate step is necessary, corresponding to weaving the cords (Figure 2 (b)). These processes will be explained in more detail in this dissertation.

Dipping is the most crucial process used at C-ITA and consists of coating textile fibers, allowing sufficient bonding between the fiber and the surrounding rubber matrix in the tire. In this way, an important fact that should be focused on is the content of coating that is applied to the fiber, not only because of safety issues but also to not overuse materials (Pratapsi, 2017; Santos, 2018).

There are three methods used in C-ITA to measure the Dip Pick-up (DPU), i.e., the mass fraction of dipping solution coated on the cords: Weighing Method (WM), the Wet Chemical Method (WCM), and the Time Domain Nuclear Magnetic Resonance analysis (TD-NMR). The TD-NMR equipment must be calibrated for each material, and usually, the chemical method provides the DPU values as a reference for the calibration curve. Previous work has already been developed to build the calibration curves for the materials produced in C-ITA. The curves developed for all materials until now were obtained for Resorcinol-Formaldehyde-Latex (RFL) dipping solution. However, in partnership with Kordsa, Continental has developed a more sustainable dipping solution, Cokoon, to replace the RFL since its composition contains toxic substances. This eco-friendly dipping solution has already been implemented on Rayon fibers, and although two calibration curves for TD-NMR have been developed, neither one was approved due to problems in their validation. The main goal of this dissertation was to calibrate the TD-NMR for Cokoon dipped Rayon with subsequent successful validation of the calibration curve. Thus, the first part of the project focuses on understanding what problems prevent the validation of the previous curves. Several factors may be at the root of the problem; however, a more intensive study will be devoted to the WCM since, until now, the DPU values used as a reference for the TD-NMR calibration curves were provided by this method. Therefore, it is essential to understand the reliability of this method for this new dipping solution and to find the best Dip Pick-up determination technique to use as a reference for the calibration curve on TD-NMR.

1.3 Contribution of the author to the work

This project will continue the study of the Wet Chemical Method started by Neves (2022), who realized that the method might not be the most suitable for the Cokoon dipping solution.

In the first phase of this master dissertation, an analysis of the WCM was done, and after comparing the data with the Weighing Method and Kordsa-Chemical Method, it was proven that the WCM does not work for the new formulation.

In the second part of the project, a new calibration curve was obtained in the TD-NMR for the Rayon fabric treated with the Cokoon using the WM to provide the DPU values. The validation of the curve was not possible due to the lack of reliable samples, but in the future, it can be validated with new samples when the material starts being produced again, saving the company time.

1.4 Organization of the dissertation

This work is divided into seven main chapters, which are presented next:

1. **Introduction.** This chapter includes some information about the company where this dissertation was developed as well as the main goals and contributions.
2. **State of the art.** Contextualization of the importance of a tire and the materials used by C-ITA for textile reinforcement. Explanation of the production processes and methods used for quality control.
3. **Materials and Methods.** The methodology and technology used during this project are explained in this chapter.
4. **Results and discussion.** Results are presented along with the respective analysis.
5. **Conclusion**. Here, the main conclusions are summarized in this chapter.
6. **Assessment of the work done.** This chapter evaluates how successful this thesis was, pointing out the goals achieved. Besides that, some suggestions are given for future experiments that can be performed.
7. **Bibliography.** List of the references used in this project.

2 State of the art

This chapter will present the necessary theoretical background for a good understanding of this project. Therefore, the tire field is introduced, including its composition and functions. The textile reinforcements included in the tires will receive special attention, where the production process of these will be described, as well as the methods and equipment used for the project.

2.1 Tires

Tires are more than just rounded pieces of rubber. They are advanced engineering products, and the mystery of them performing many functions simultaneously results from their extensive range of specialized components (Figure 3) (Burak Erman, 2013; Nakajima, 2019).

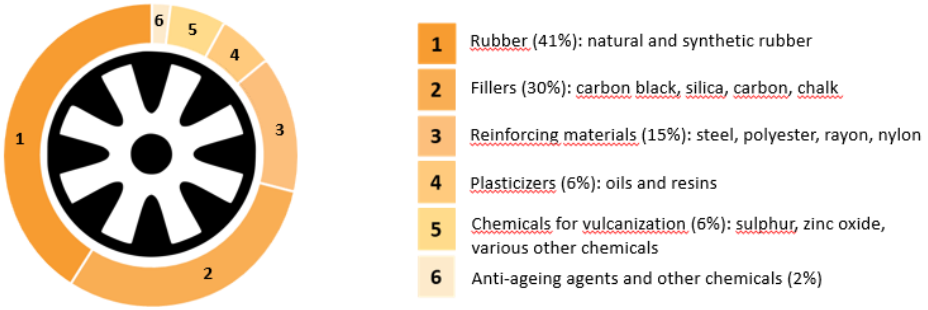

Figure 3. Composition of a modern tire. Adapted from (Continental, 2013 / 2014).

Tires are designed to meet some goals like absorbing road irregularities, supporting the vehicle load, offering good road friction in both wet and dry conditions, and providing the vehicle interface with the road. By ensuring these functions, safety and security are transferred to the passenger, which is the most crucial purpose of tires (Davisson, 1969; Lugner, 2019).

Nowadays, the main tires in the industry are the radial ones, which gained popularity in the 1970s. These tires can be categorized as primary components: carcass plies, beads, belts, and tread, and secondary components like chafers, flippers, and breakers. Primary components are responsible for the most important tire characteristics like geometric shape and stress capacity, and the secondary protect the primary components from high-stress concentration (Britannica, 2016; Davisson, 1969).

Figure 4 shows the individual components of a tire, and their properties and functions are also explained.

Figure 4. Tire components from a radial tire of Continental. Adapted from (Continental, 2022b).

The tread is of particular significance since it must ensure high mileage, good adhesion between the road surface and the tire, and water expulsion. These requirements allow the vehicle to drive, brake, and corner with minimum noise generation and low heat buildup. Tread components consist of natural and synthetic rubber (Burak Erman, 2013; Continental, 2022b; Rodrigues, 2017).

The layer that sits directly below the tread is the jointless cap plies, consisting of nylon cords cured in rubber. Their function is to enable high speeds. Relatively to the steel cord belt plies, they provide directional stability and a decreased rolling resistance by using high-strength cords (Continental, 2022b; Rodrigues, 2017).

Concerning the inner part of the tires, the textile ply or carcass comprises textile cord and rubber, specifically rubberized Rayon or polyester, placed radially. The carcass holds the air pressure, preventing tire deformation and, thus, giving the vehicle better handling and stability (Britannica, 2016; Continental, 2022b).

The inner liner is a thin composite with a special formulation of butyl rubber, a material with low permeability to gas. The liner seals the air-filled inner chamber by decreasing the permeation through the tire (Britannica, 2016; Santos, 2018).

The sidewall is made of natural rubber, and its primary function is to increase the tire's fatigue resistance by protecting the casing from scraping or other external damage (Continental, 2022b).

The tire bead is the connection between the tire and the wheel being divided into three parts: bead reinforcement, bead apex, and bead core. Bead reinforcement includes layers of textile reinforcements, nylon or aramid, that enhance the sidewall/bead area, promoting directional stability. The bead apex is made of synthetic rubber and provides additional comfort in addition to the bead reinforcement functions. Finally, the bead core is responsible for the connection

between the tire and the rim, and it is made of steel wire embedded in rubber (Burak Erman, 2013; Continental, 2022b).

The type of tire mentioned until now was radial-ply belted; however, there are two more, the bias-ply and bias-ply belted (Figure 5). These three types differ in how the reinforcing cords layers are laid or arranged in the carcass (Britannica, 2016).

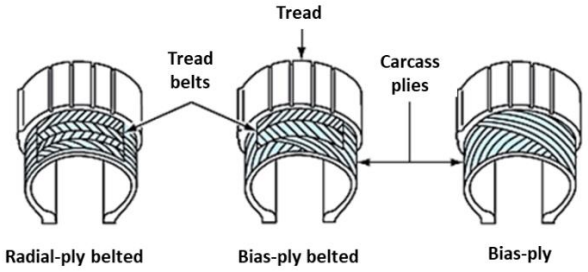

Figure 5. Different types of body ply arrangement. Adapted from (Skedsoft, n.d.).

The difference between bias-ply tires and bias-ply belted tires is the addition of another set of cords on this last type, called a belt. The belts improve the tread region's strength and stability, providing better gasoline mileage. A radial tire also has belts, but unlike the other arrangements, the cords are placed to have a 90° angle with the tire tube axis in the radial-ply structure. This allows for better steering characteristics and less rolling resistance, resulting in longer tread life and greater security against weather conditions, explaining why these tires are more expensive (Britannica, 2016).

2.2 Textile Reinforcements

For rubberized applications, the reinforcement with cords is the key element to prevent failure of the product's performance, in terms of deformation of rubber when subjected to high loads in demanding situations.

There are different terms for textile constructions with varying levels of complexity, namely filament, yarn, cord, and fabric. A filament is the simplest one, following the yarn composed of several filaments laid together, then a cord made by one or more yarns twisted together, and finally fabric. The fabric is composed of synthetic warp cords held together by weft yarns (Pratapsi, 2017).

C-ITA receives all types of fibers, and depending on the type of tire desired, the yarns are rigorously prepared, resulting in cords or fabrics, as mentioned before. For both products, it is necessary a twisting process to transform the raw materials (yarn) mentioned above into cords (Figure 6 a)) (Santos, 2018).

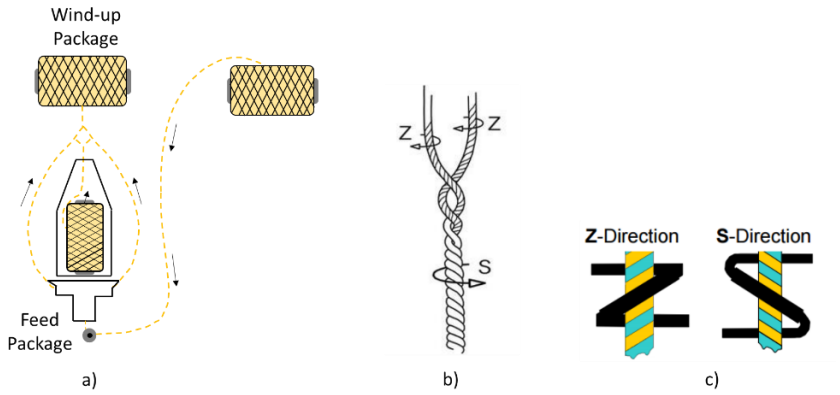

Figure 6. Greige cord production: a) twisting process; b) twisted cord; c) possible twist directions. Adapted from (Pratapsi, 2017; Rodrigues, 2017).

Twisting can be applied in two different directions, "Z" or "S", as can be seen in Figure 6 c). If the cord is turned in a clockwise direction from top to bottom, it is twisted in "Z"; if the cord is winded in a counterclockwise direction, it has an "S" twist. Usually, the yarn is twisted first in the "Z" direction and then in the "S" direction (Figure 6 b)). This process is made on a twisting machine to produce a greige cord, improving the fatigue resistance and the elongation of the textile (Silva, 2020).

Cords can also be characterized by the linear density, corresponding to the mass per 10 000 meters of cord or decitex (dtex), twist level, and cord construction. The twist level is the number of twisting turns per meter on the cord, and the cord construction represents the number of yarns in a cord and how they are twisted (Silva, 2020).

In the case of fabrics production, a weaving process is necessary, where a variable number of bobbins of the cord are joined to create a fabric. Figure 7 shows how the weaving machine works.

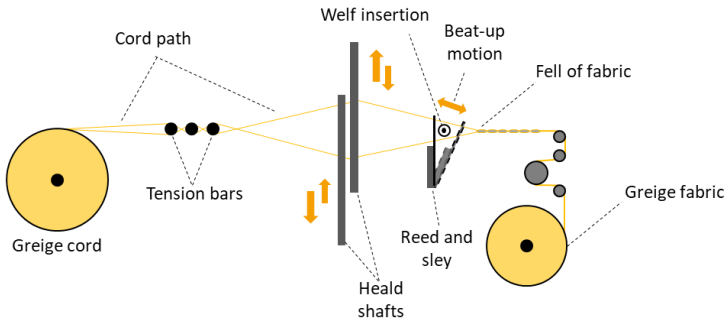

Figure 7. Weaving process. Adapted from (Bilisik, 2011).

2.3 Fibers

The textiles produced in this company are made of nylon, aramid, polyethylene terephthalate (PET), and rayon. Besides these textiles, C-ITA also produces hybrid cords, using nylon and

aramid to achieve better properties. These fibers are mainly applied as the carcass and cap-ply reinforcements in tire design. Polyester and Rayon are mainly used in the carcass of a tire and are placed radially from bead to bead. They act as a primary reinforcement and strength member of the tire. On the other hand, nylon and aramid fibers are placed in the cap-ply providing additional stiffness and low shrinkage to the tire. These properties prevent the deformation of the tire (Lindenmuth, 2006).

Nylon is a synthetic long-chain polymer characterized by the presence of amide groups that are produced by continuous polymerization. Besides, a wide diversity of nylon polymers exists, only two are applied in tire manufacture, nylon 6 and nylon 6,6. These two fibers have good strength, high heat and fatigue resistance, and low moisture sensitivity (Gupta, 2013; Nokian Tyres Plc., 2017).

PET just like nylon, is a synthetic long-chain polymer and is produced by continuous polymerization between dimethyl terephthalate (or terephthalic acid) and ethylene glycol. These fibers should present an excellent resistance to elasticity throughout the tire's lifetime. It is not as resistant to heat as nylon or Rayon (Lindenmuth, 2006; Westgate & Gillick, 2008).

Aramid is an aromatic polyamide with high strength, stiffness, and good heat resistance. These cords present high tenacity and are two to three times stronger than PET and Nylon. Due to its lightweight, the primary usage of this cord in a tire is for belt or stabilizer ply material as an alternative to steel cord. This material has disadvantages like its high cost and the difficulty of cutting it (Rocha, 2019; Santos, 2018).

Rayon was the first manufactured cellulosic fiber and is made by wet spinning. This material is an excellent choice for tires due to its stable dimensions, heat resistance, and good handling characteristics (Gupta, 2013; Lindenmuth, 2006). However, this compound has some issues like high sensitivity to moisture and environmental damage associated with its manufacturing. The fiber becomes significantly weaker when wet, losing strength temporarily. Therefore, it must be handled with care during its usage (Gupta, 2013; Lindenmuth, 2006).

2.4 Dipping Process

The cords and fabrics obtained by the twisting and weaving processes in C-ITA are not ready to perform their function. Textiles do not have a proper adhesion to the rubber without any treatment due to the incompatibility between both materials. This lack of compatibility results from a significant difference in the polarity between the greige cords and rubber. Textiles are characterized by a polar character, while rubber is non-polar. Their interaction is weak, requiring a final step to coat the greige cords with a dipping solution, allowing sufficient bonding between the fiber and the surrounding rubber matrix (Louis et al., 2014). Figure 8

shows how the dipping solution for coating textile reinforcements acts like an interface between the fiber and the rubber.

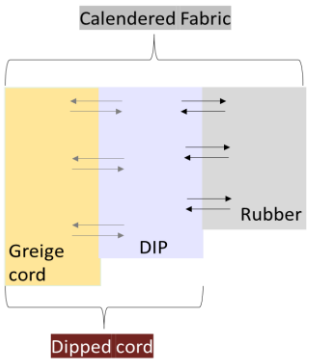

Figure 8. Adhesion Interchange Mechanism. Adapted from (Santos, 2018).

C-ITA has two different dipping machines, one designed for cords, Single-end, and another for fabric, Zell. Figure 9 and Figure 10 show the schematic of the Single-end and a Zell machine, respectively. The name of the Single-end machine is related to the fact that the greige cords unwind in the same place that the dipped cords wind (left side). In this machine, the cord goes through different stretch levels on the tensioning rollers, then are dipped in the first bath, and finally, the heat treatment takes place in the first and second ovens, where the exposure time is a fundamental property. In the first oven, the dipping solution is dried, and the second oven is responsible for hot-stretch the cord, where the product acquires its final properties. In case of a material that needs a pre-dip, after the second oven, the cord passes in a second bath and then in two more ovens (3rd and 4th), where the 3rd oven acts as the second dry zone and the 4th one as a normalizing oven (Santos, 2018; Silva, 2020).

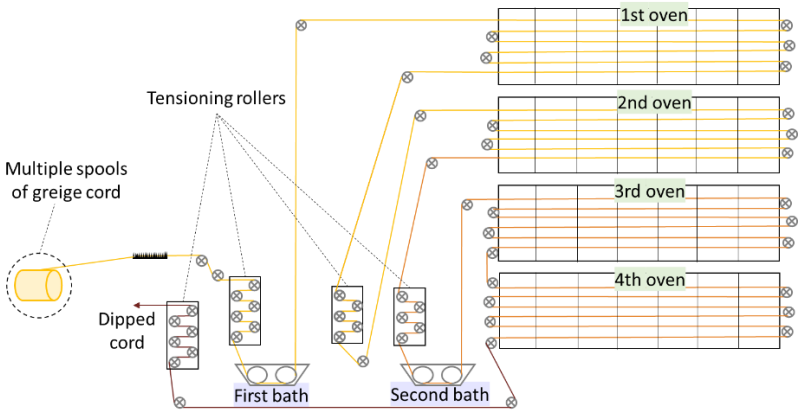

Figure 9. Schematic plant of Single-end equipment. Adapted from (Santos, 2018).

The Zell machine works very similarly to the Single-end machine, differing in the number of ovens since it contains three more, and the final fabric product does not wound up on the same side as greige fabric. Furthermore, just one roll can be dipped at a time, while in the Single-

end device, multiple cords are dipped simultaneously (multiple spools per batch) (Pratapsi, 2017; Rocha, 2019).

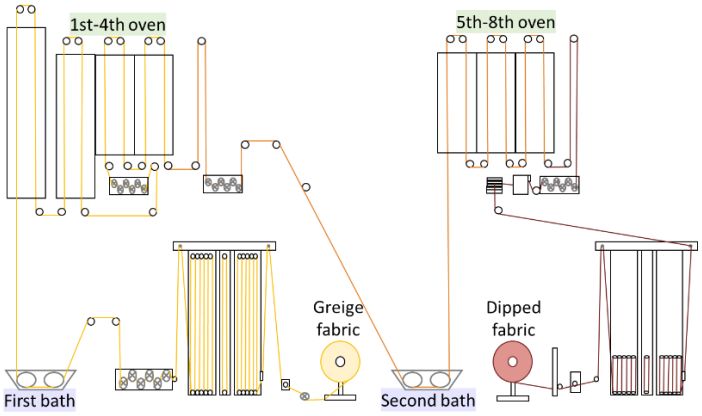

Figure 10. Schematic plant of Zell equipment. Adapted from (Santos, 2018).

2.4.1 Resorcinol-Formaldehyde-Latex (RFL) dipping solution

The most common dipping solution used in cords is the Resorcinol-Formaldehyde-Latex (RFL), which is constituted of water, a latex emulsion, and a resin that creates mainly covalent bonds, forming a matrix. RFL is the conventional dipping solution used in C-ITA. The latex used is styrene-butadiene-2-vinyl pyridine (VP latex), and if this compound is used alone, it would interact with the rubber compound but not with the fiber. Thus, it is vital to add a resin made of resorcinol and formaldehyde (RF resin) (Figure 11), responsible for enhancing the bonding to the cord (Louis et al., 2014).

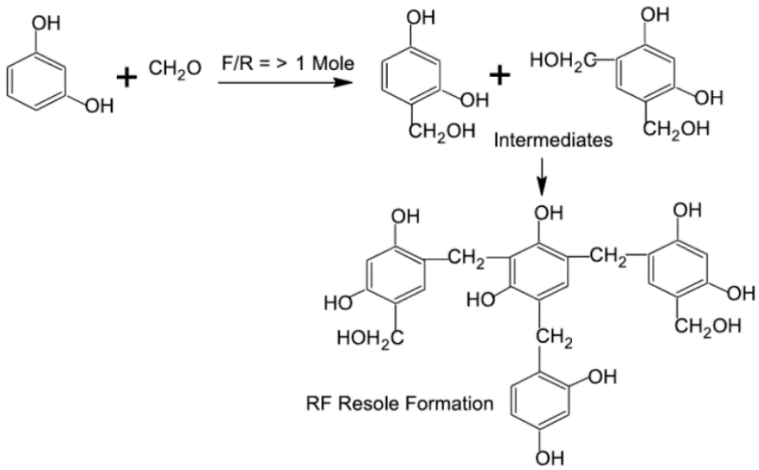

Figure 11. The reaction of resorcinol and formaldehyde to produce Resoles RF resin (Durairaj, 2005).

The formula for adhering RF resins to Rayon was suggested by Skeist (1990) (Figure 12).

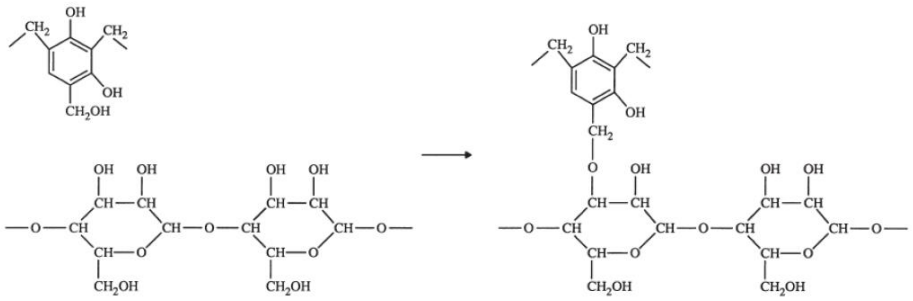

Figure 12. Moult's theory of adhesion of RFL to Rayon tire cord (Skeist, 1990).

Each type of fiber requires different formulations with proper Solid Content (SC). Furthermore, the cords can pass through one or two dipping solutions depending on the reactivity of the materials. In the case of nylon or Rayon, a traditional treatment with RFL dipping solution is sufficient because their reactivity is high enough. However, for aramid and PET, a primary bath is required due to its extremely non-reactive properties. Pre-dip uses a solution of epoxy resin and isocyanate that is responsible for the activation of the cord, bonding to the dipping solution. Some suppliers of C-ITA already make this step by using an oil finish in yarns that will allow the functionalization of the cord (Silva, 2020).

2.4.2 Cokoon dipping solution

Recently, C-ITA has been studying a more sustainable formulation named Cokoon to reduce the environmental impact caused by the toxic substances in RFL dipping solution. The Cokoon dipping solution is free of resorcinol and formaldehyde. The composition of this sustainable formulation consists of water, three different latexes, a blocked isocyanate, and an epoxy group-containing compound.

- **Blocked isocyanate**

Isocyanates are renowned for their high reactivity and selectivity towards various functional polymers since, at room temperature the isocyanates react immediately with hydroxyl containing compound, for instance. Therefore, to be possible to store these components without the occurrence of undesirable reactions, it is used a blocking agent that masks the isocyanate group. Thus, the new compound is seemingly inert at room temperature, recovering its reactive isocyanate functionality at elevated temperatures when the deblocking temperature of the blocking agent is reached. Usually, the blocking reaction occurs with a compound containing an active hydrogen and there is a large variety of blocking agents that comprise at least one active hydrogen atom in the molecule (Avar et al., 2012; Rolph et al., 2016).

In the Cokoon dipping solution, the isocyanate used is the 4,4′-methylenediphenyl diisocyanate (MDI) blocked with ε-caprolactam (Figure 13) due to its good performance in surface coating.

The deblocking reaction occurs at temperatures of 155 - 180 ℃ (Lee et al., 2005), where the ε-caprolactam is regenerated with subsequent liberation of the reactive MDI since the hydrogen bond on the nitrogen is very weak. After the deblocking temperature it is achieved, a faster curing process occurs (Frisch, 2002; Klempner, 1998).

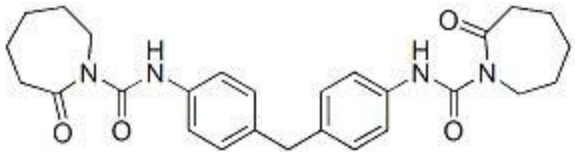

Figure 13. ε-Caprolactam blocked Methylene diphenyl diisocyanate (Gloriaful, 2022).

- **Epoxy Resins**

The epoxy group present in the Cokoon dipping solution belongs to a resin-forming component based on 1,2,3-Propanetriol and glycidyl ethers, which are environmental-friendly, feasible, and easily accessible. The 1,2,3-propanetriol-diglycidyl-ether (PTGE), for instance, it is used as a reactive diluent for epoxy resins like this one (Xu et al., 2015). The versatility of these resins is related to the significant reactivity of the epoxy group. During the curing process, when a surface containing hydroxyl groups like Rayon contacts the epoxy group, adhesion occurs through covalent bonds: the resin acts as a strong adhesive (Xu et al., 2015).

2.5 Dip content in textiles and quality control

Dip content is a crucial parameter in economic and quality terms since an excess of dipping solution results in overuse and environmental concerns, and a lack of it causes adhesion problems in tire performance, mainly providing carcass failure.

For all reasons mentioned before, it is easy to understand that a reliable method is necessary to determine the Dip Pick-up of the dipped cords. The Wet-Chemical Method, Weighing Method, and the TD-NMR equipment are used to measure the DPU in C-ITA. The DPU is defined as the mass ratio between the dip attached to the cord and the greige cord or dipped cord. Since the WCM is the conventional method used in C-ITA and a new dipping solution has been studied, it is necessary to evaluate the reliability of this method as well as the other methods used in the company like the Weighing Method.

2.5.1 Weighing Method

The WM compares the weight of the dipped cord with the weight of the greige cord, allowing to obtain the mass of the dip retained by the cords to calculate the DPU.

This method is avoided in C-ITA since it has associated errors and is very sensitive to the moisture on the fibers. However, the WM is commonly used for some fibers, like PET, which have a very low hygroscopic nature. For materials highly hygroscopic, like Rayon, the moisture

can affect the results, so the cords are cut into laces and dried before measuring the weight. However, the WM has advantages relative to the WCM as it does not need to dissolve the fiber with environmentally harmful chemicals and is less time-consuming.

2.5.2 Wet Chemical Method

This method is determined by differences in mass (gravimetric method). It consists of dissolving a fiber in a suitable solvent with subsequent filtration of the solution to recover the dipping solution residue. Then, the result of filtration is dried and finally weighed, allowing to calculate the DPU.

WCM has a high number of errors associated, and besides that, the high time required for this method makes it impracticable for quality control for some fibers, such as aramid and PET. For these reasons, the most commonly used method in the Production Department (PD) is Time Domain-Nuclear Magnetic Resonance analysis since it gives much faster results. However, the TD-NMR equipment needs a calibration curve for each material, and usually, the WCM provides the DPU reference values.

- **Commonly Used Acidic Reagents to dissolve regenerated fibers**

In order to reevaluate the WCM, a survey of the most commonly used solvents in the industry for dissolving Rayon fibers was conducted to understand if the one used in C-ITA, constituted by zinc chloride and formic acid, is appropriated (Cao et al., 1995). According to the literature, zinc chloride is one of the most widely used metal salts for dissolving fibers and has proven to be efficient in dissolving Rayon (Gao et al., 2017; Zhang et al., 2019). However, the hydrolysis of these fibers is only achieved in an acidic medium. Many acids, due to its small molecular size, can penetrate the crystalline structure of cellulose. To achieve good hydrolysis, the individual fibrils of cellulose are broken through the destruction of their internal hydrogen bonds (Figure 14 a)). When this happens, the individual glycoside bonds are exposed to the catalyst (zinc chloride), resulting in water-soluble and stable zinc-cellulose complexes (Figure 14 b)) (Cao et al., 1995). These complexes can be hydrolyzed in acid solution more quickly than solid cellulose.

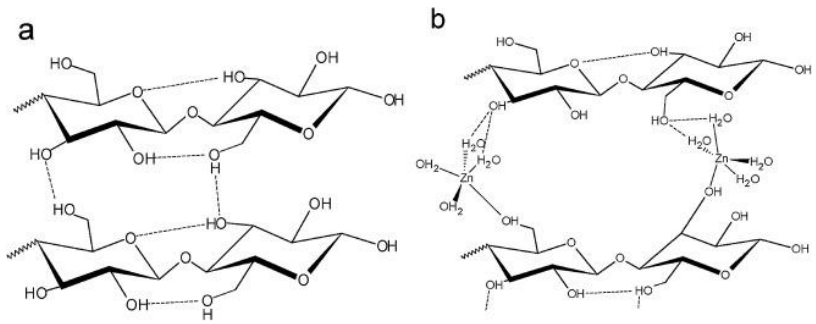

Figure 14. a) Hydrogen-bonds in cellulose. b) The hydrate zinc chloride broken up hydrogen bond between polymer of glucose. (Zhang et al., 2019).

Gao et al. (2017) studied the solubility of different regenerated cellulose fibers in acidic reagents commonly used in the dissolution method. Viscose Rayon was one of the cellulose fibers studied, and some of the possible acids used and the conditions needed are presented in Table 1. Besides three different solvents being tested, the authors focused their investigation on the formic acid/zinc chloride system. The conclusions drawn by the authors of the article were that the optimal conditions for the complete destruction of Rayon from zinc chloride and formic acid correspond to a temperature of 70 ºC for 1 h. This conclusion proves that the conventional C-ITA method is reliable for dissolving Rayon fibers since the conditions used are the same. Therefore, the problems that can occur when using this method can only result from the interaction between the dipping solution and the reagents used to dissolve the fibers (Gao et al., 2017).

Table 1. Dissolution of regenerated cellulose fibers in acid reagents and respective experimental conditions (Gao et al., 2017)

Reagents	Oscillation	Temperature / ºC	Time / min	Solubility
36 - 38 % HCl	No	70	-	Dissolved Quickly
36 - 38 % HCl	Yes	RT*	30	Dissolved
60 % sulfuric acid	Yes	RT*	30	Dissolved
Formic acid/zinc chloride	Yes	70	20	Dissolved

*RT – Room Temperature

2.6 Time Domain-Nuclear Magnetic Resonance Method (TD-NMR)

The TD-NMR method is more advantageous compared to the other two methods, as it is much less time-consuming and produces high-quality results with a low associated error (Bruker, 2015).

The TD-NMR is based on relaxometry and provides only time-domain signal, i.e., no chemical information is given. It has been proved to be helpful to study the dynamical properties of polymer chains through the measurement of physical properties like signal amplitude (Besghini et al., 2019).

As is well known, each atom has protons and neutrons in its nucleus that spin around an axis. This property is named spin angular momentum. The spin angular moment is characterized by the principal quantum number (n), meaning it can only assume the value ± ½ (Britannica, 2019).

TD-NMR analysis involves the detection of a signal using a spectrometer. During the process, there is a perturbation of the equilibrium state of protons (^{1}H); they are excited by a radio frequency in a magnetic field B_0, generated by the magnetic unit inside the spectrometer. The

samples introduced into the unit have an NMR active nuclei (^1H) with a non-zero spin, which causes a magnetic moment. The spins of the hydrogen nuclei (parallel and antiparallel to the field) on the sample change the normal orientation due to the polarization generated by the field (Figure 15 a)). Thus, it arises a net magnetization vector M_0 with B_0 (Figure 15 b)). Through the excitation caused by the radio frequency pulses, a magnetic field B_1 oriented perpendicular to B_0 appears (Figure 15 c)) and the orientation of the net magnetization M_0 changes to M. After the radio frequency pulses are deactivated, the spin system slowly releases energy. The NMR signal decays over time as spins return to equilibrium, which is called relaxation. Two types of relaxation occur: spin-lattice relaxation (longitudinal relaxation) and spin-spin relaxation (transverse relaxation) characterized by relaxation time T1 and relaxation time T2, respectively. The longitudinal one results from the release of energy, manifested by the gradual recuperation of the magnetization vector in the z-axis direction of B_0. The spin-spin relaxation results from the interaction between the spins that co-occur as the releasing energy. As a result of this interaction, a dephasing in the transverse direction arises, called spin-spin relaxation (Figure 15 d)) (Besghini et al., 2019; Li & Ma, 2021).

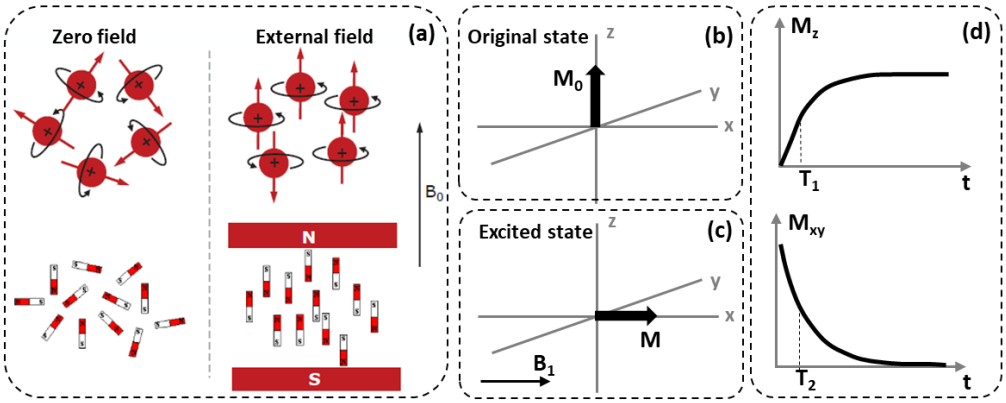

Figure 15. Demonstration of the basic working principle of NMR. Adapted from (Li & Ma, 2021).

Relaxation time T2 should be obtained by flipping the magnetization on the xy plane with a single π/2 pulse and then analyzing the free induction decay (FID). However, field inhomogeneities produce a much shorter decay time for low-field devices, indicated as T2* (Figure 16). Thus, more complex sequences, like Hahn-Echo (HE) experiments, must be applied to remove the field's effect. HE experiments depend on the formation of spin echoes and consist of an application of a π/2 pulse followed by π pulses that relocate the dephasing of spins caused by the field inhomogeneities with the formation of an echo. Therefore, the first pulse, 90 °, causes an FID when the equipment detects radiation that is emitted in this decay curve. At the end of this pulse, the signal emitted by the protons is at its maximum intensity. However, the intensity decreases rapidly because the protons return to their original energy state (Besghini et al., 2019; Li & Ma, 2021).

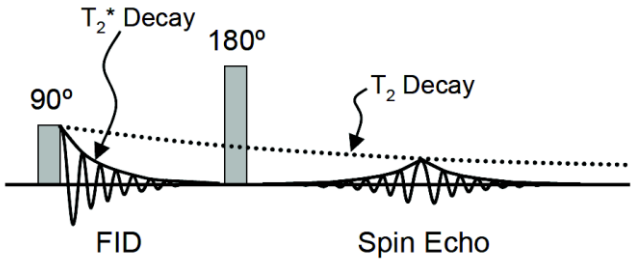

Figure 16. Reorientation of magnetic field inhomogeneity (Bruker, 2015).

The relaxation time T1 is a function of molecular motion and field strength and is characterized by magnetization recovery along the static field direction axis. The longitudinal relaxation implies an energy exchange between the spin system and the environment. The energy exchange only is allowed if the energy gap between the high-energy and low-energy spin states overlaps with the vibrational and rotational energies (Besghini et al., 2019).

Usually, a five-times T1 between each scan is necessary to allow a complete return to the equilibrium state along the z-axis, corresponding to the direction of the static magnetic field. So, increasing the field strength results in a lower T1, meaning a decrease in the experimental time (Besghini et al., 2019).

The TD-NMR equipment acquired by the company uses the Spin-Echo applications to quantify the amount of dip on the cord. The determination of DPU is based on different relaxation properties of the materials present in the sample cord and the dipping solute, in this case. Since the dip has a shorter relaxation time (Bruker, 2015), the signal obtained after the 180 ° pulse will be generated by the fiber sample, while in the 90 ° pulse, the signal is generated by the fiber plus the dipping solution. Thus, the dip amount is measured by the difference between these two signals, as seen in Figure 17. (Aubin et al., 2020; Bruker, 2015).

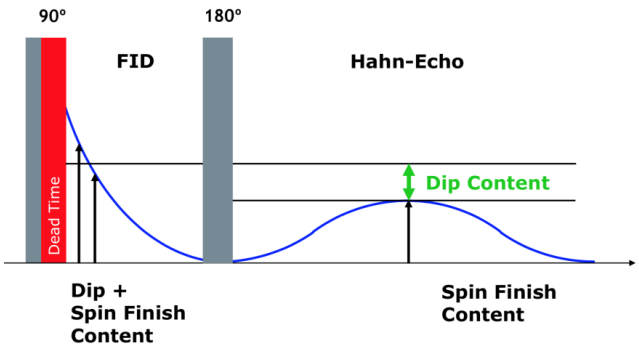

Figure 17. Schematic representation of the DPU measurement by TD-NMR (Bruker, 2015).

The main difference between the usual TD-NMR method and this same method used in C-ITA is that both dip and fibers are solid instead of solid and oil-type materials. However, depending on the supplier of yarns of this company, some of them have oil in their composition. So, an

application and optimization in software device was made to remove the signal associated with the spin-finish oil from yarn, resulting in dipping solution measurement only (Bruker, 2015).

2.7 Assessment of previous work

As mentioned earlier, the TD-NMR was a major and essential acquisition for C-ITA. Many dissertations have already focused on calibrating this equipment for the different materials produced at this company. In the previous master thesis, a calibration curve was obtained for Cokoon dipped Rayon (Figure 18) (Neves, 2022). However, this curve was not validated due to the significant difference between DPU measurements obtained by TD-NMR and WCM for fifteen samples collected (Neves, 2022).

Neves (2022) also performed a power test to prove that only 15 samples are needed to validate the TD-NMR calibration curve for Cokoon dipped Rayon.

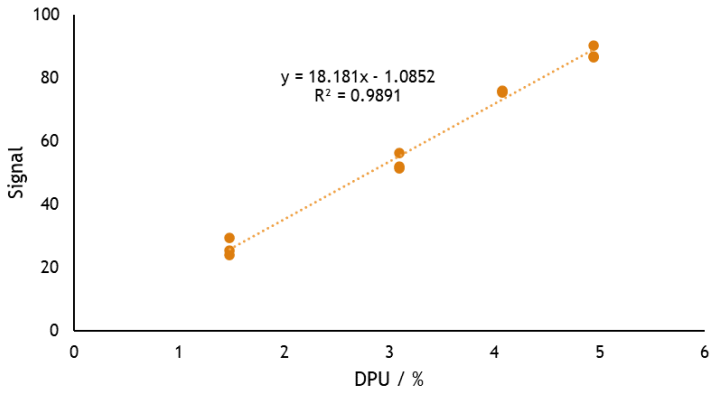

Figure 18. Cokoon dipped Rayon's calibration curve (Neves, 2022).

This current Master Thesis focuses on developing a new calibration curve for this material as well as a study of the other methods used to measure the amount of dip on the fiber.

3 Materials and Methods

3.1 Experimental planning

This chapter presents all the materials and methods used throughout the work. The material studied was Rayon from two suppliers with a different linear density (Table 2). The Rayon provided by supplier A is dipped with Cokoon, and the one delivered by supplier B with RFL.

Table 2. Standard cords characteristics

Textile	Supplier	Linear density / dtex	Cord construction
Rayon	A	1840	1840 x 2
Rayon	B	2440	2440 x 2

The first part of the project focuses on the study of the WCM. For this purpose, three different methods used to determine the Dip Pick-up of Rayon were compared: WCM and WM used at C-ITA and the chemical method utilized by Kordsa. These methods were applied to Rayon dipped with RFL and Cokoon to determine if the results varied similarly for the two dipping solutions. The main purpose was to understand the reliability of WCM when it is used for Cokoon dipped Rayon.

The second part of the project was to continue the work developed so far of calibrating the Time Domain Nuclear Magnetic Resonance equipment for Cokoon dipped Rayon.

3.2 Sample preparation

The samples correspond to spools with dipped cords, prepared in a machine called Laboratory Dipping Unit (LDU) (Figure 19). This machine is very versatile since it can replicate the treatment applied to cords or fabrics in Production Dipping Units (PDU), shown in Figure 9 and Figure 10, on a laboratory scale. Through the LDU, it is possible to test different materials, dipping solutions, and variables.

As can be seen in Figure 19, this unit has only four ovens. Thus, to reproduce the Zell machine of PDU, the number of passages in the ovens (loops) is changed to achieve the same exposure time, according to each temperature zone. The operation conditions such as velocity, stretch levels, and temperatures are also adapted from those used in PDU since previous work has already focused on scaling down these conditions.

For Rayon, only one bath is needed. Cokoon formulations are prepared in the Chemistry Laboratory, and the pH and SC must then be measured to verify that they are within the specified range. RFL dipping solution can also be prepared in the lab; however, if it is used in

Production Department, the amount needed for use in the LDU can be collected. In the case of the RFL dipping solution for Rayon, only the one produced in PD should be used since, when made in the Laboratory, it tends to coagulate.

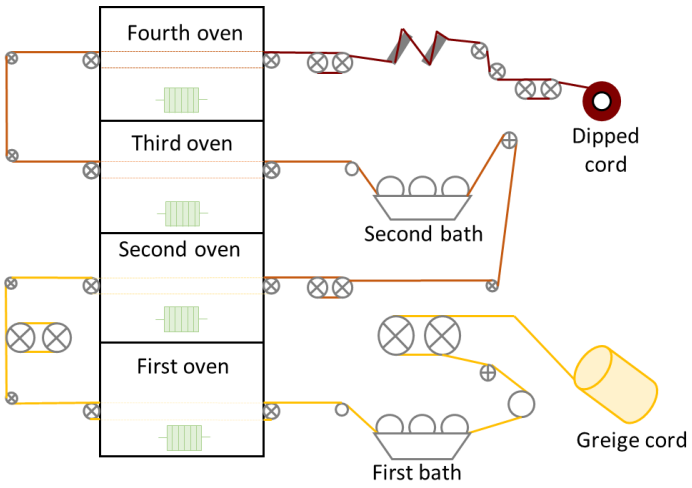

Figure 19. Scheme of the LDU machine.

The LDU can also be used without the dipping solution to maintain the materials' temperature, stretches, tensions, and velocity conditions. This process consists of thermofix the greige cords. Thus, there is an approximation between the greige cord and dipped cord in terms of mechanical properties since the only difference is the absence of dipping solution.

3.3 DPU measurement

In this project, four methods were used to determine the amount of DPU; three are used in C-ITA: WCM, WM, and TD-NMR. In addition, trials were also performed with the Kordsa-Chemical Method (KCM).

3.3.1 Weighing Method

This method compares the weight of the cords before and after the dipping process. To minimize the errors associated with the indicated method, instead of directly weighing the greige cord, first, it is thermofixed in the LDU and then weighed.

The procedure involved preparing ten replicas from thermofixed cord and dipped cord with 10 meters each (Figure 20). The samples were tied up in the form of laces and dried in the oven for at least 1 hour and a half at 105 °C. The dried samples were weighed one at a time, and the DPU per greige cord, $\mathrm{DPU}_{\text{per greige cord}}$, was determined by Equation 1, where $m_{\text{dipped cord}}$ corresponds to the weight of one dipped sample and $m_{\text{greige cord}}$ to the weight of one greige sample. The $\mathrm{DPU}_{\text{per greige cord}}$ corresponds to the mass of dipping solution recovered per mass of greige cord.

$$\mathrm{DPU}_{\text{per greige cord}} = \frac{m_{\text{dipped cord}} - m_{\text{greige cord}}}{m_{\text{greige cord}}} \times 100 \quad (1)$$

Figure 20. Weighing Method samples - dipped Rayon cord with: a) Cokoon dip and b) RFL dip.

3.3.2 Wet-Chemical Method and Kordsa-Chemical Method

The chemical methods used in C-ITA and Kordsa allow the measurement of the amount of dip that remains attached to the cord by its dissolution in a suitable solvent (Table 3). The procedure followed for these methods is presented in Figure 21.

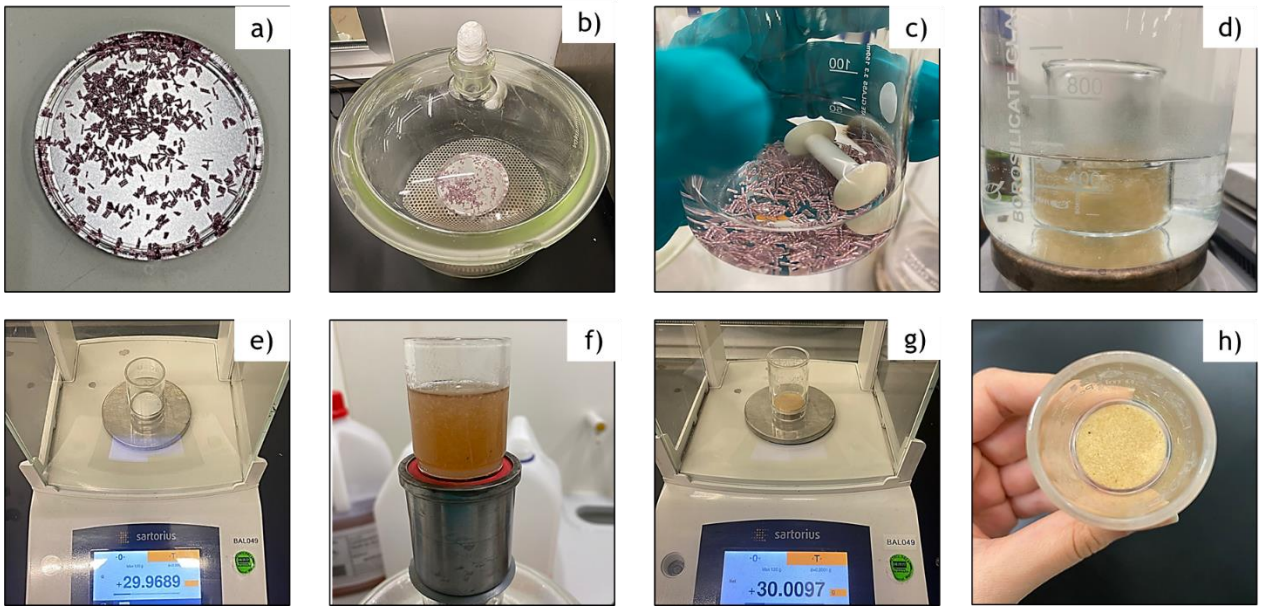

Figure 21. Wet-Chemical Method procedure for Cokoon dipped Rayon.

The dipped cord was cut into small pieces (Figure 21 a)), until 1 to 2 g was reached and dried in the oven, according to Table 3. The sample was cooled down until room temperature (Figure 21 b)) and weighed in a beaker (Figure 21 c)). After one hour of dissolution (Figure 21 d)) with the appropriate solvent and temperature, the resulting mixture was filtrated through a glass filter crucible (Figure 21 e) and f)) and washed with the corresponding heated fluids (Table 3).

Finally, the crucible with the dipping solution was dried in the oven and weighed (Figure 21 g)). Equation 2 was used to determine the $\mathrm{DPU}_{\text{per greige cord}}$. Thus, the m_{dip} is calculated by the difference between the mass of the crucible with the dip, after drying in the oven (m_3) and the mass of the crucible (m_2). The $m_{\text{greige cord}}$ corresponds to the initial mass of dipped cord placed in the beaker (m_1) minus the m_{dip}.

$$\mathrm{DPU}_{\text{per greige cord}} = \frac{m_{\text{dip}}}{m_{\text{greige cord}}} \times 100 = \frac{m_3 - m_2}{m_1 - (m_3 - m_2)} \times 100 \quad (2)$$

This procedure is performed at least three times for each sample to obtain three consistent results, with a standard deviation under 0.4 %, where the DPU is the mean of the three samples of Dip Pick-up.

Table 3. Reagents and experimental conditions used in the Wet-Chemical Method and Kordsa-Chemical Method

	Wet-Chemical Method	**Kordsa-Chemical Method**
Dissolution agent	50 mL of formic acid (98 %) with zinc chloride	120 mL of sulfuric acid, 72 %
Washing Fluid	50 mL of formic acid, 85 %; 50 mL of water	50 mL of acetone; 50 mL of water
Dissolution Temperature / °C	70	40
Oven temperature / °C	105	121
Time in the oven before dissolution / min	60	30
Time in the oven after dissolution / min	120	30

3.3.3 TD-NMR

The TD-NMR measurements were conducted on a Bruker equipment (Minispec mq20) (Figure 22). The equipment is very versatile and is controlled by Minispec Plus software that allows the user to perform multiple calibrations, change reference values at any time, validate calibrations, and measure samples with the previously established calibrations.

Bruker developed an application for C-ITA to measure the Dip Pick-up on cords. This process and its conditions and parameters were properly studied and optimized by the company's technical experts that manufactured the equipment to make the measurements efficient. The definition of parameters for this software, like the number of scans, are present in Figure A.1 from Annex A.

Figure 22. TD-NMR device: Minispec mq20 from Bruker.

To measure the DPU in this device, it is required to prepare the sample. Currently, there are two available methods, the traditional one, and the new cutting method. In the traditional method, the dipped cord must be tied up in a bow form, while in the new method, the samples are cut into small pieces. In this project, the new method was chosen for the Rayon material due to its simplicity and practicability.

The procedure of this method involved weighing the tubes with the lid on ($m_{\text{tube+lid}}$) and cutting the dipped cord into small pieces until a weight of 0.5 g is reached for each tube. Then, the samples are introduced into the tubes; these are dried in the oven, without the lids, for at least 1 hour at 105 ºC. After, the lids are placed on the tubes, which are then cooled to room temperature and then reweighed ($m_{\text{tube+lid+sample}}$). To measure the samples in the TD-NMR, these are heated in device support for five minutes at 40 ºC. Finally, the samples are measured in the TD-NMR device three times each.

All this procedure must be handled with gloves to avoid contamination of the cords and tubes since the TD-NMR signal are very sensitive to impurities. In addition, the readings on the device are also affected by moisture, which is why the lids are placed on the tubes immediately after drying in the oven.

When this method is used, it is necessary to convert the value of DPU from dipped cord ($\text{DPU}_{\text{per dipped cord}}$) (Equation 4) to $\text{DPU}_{\text{per greige cord}}$ (Equation 3), combining these two equations with Equation 5, since the TD-NMR equipment measures the Dip Pick-up per dipped cord.

$$\text{DPU}_{\text{per greige cord}} = \frac{m_{\text{dip}}}{m_{\text{greige cord}}} \times 100 \tag{3}$$

$$\text{DPU}_{\text{per dipped cord}} = \frac{m_{\text{dip}}}{m_{\text{dipped cord}}} \times 100 \tag{4}$$

$$m_{\text{greige cord}} = m_{\text{dipped cord}} - m_{\text{dip}} \tag{5}$$

Combining the equations above (Appendix A.1), Equation 6 is obtained:

$$\mathrm{DPU}_{\text{per greige cord}} = \frac{\mathrm{DPU}_{\text{per dipped cord}}}{100 - \mathrm{DPU}_{\text{per dipped cord}}} \times 100 \quad (6)$$

- **Calibration Curve**

The calibration of this device needs at least four different points. These points correspond to four cords with a specified amount of dip related to the DPU target range of the material. C-ITA specified this range and, in the case of Cokoon dipped Rayon, the Target (T), the Low Target Limit (LTL) and the Upper Target Limit (UTL), corresponds to 3.5 %, 2 % and 5 %, respectively. The dipped cords are obtained in the LDU machine, and each formulation is obtained by trial and error based on the calculation of the SC. However, the Dip Pick-up of each sample was only known after its measurement through the WCM, which is why, most of the time, the process involves dipping more than four cords until the desired ones are obtained. Then, these values are used as a reference to compute the calibration curve. The four different concentrations should be well distributed within the followed tolerance range:

A – Between LTL – 1 % and LTL;
B – Between LTL and T;
C – Between T and UTL;
D – Between UTL and UTL + 1 %.

For Rayon, according to continental standards, the values of DPU used to obtain the calibration curve were determined and arranged using the pre-established range present in Table 4.

Table 4. DPU necessary for each cord of the calibration curve

Cord	LTL - 1 %	LTL	Target Value	UTL	UTL + 1 %
A	1 % - 2 %				
B		2 % - 3.5 %			
C			3.5 % - 5 %		
D				5 % - 6 %	

The calibration was performed with the Minispec Plus software developed by Bruker to measure Dip Pick-up on cords in C-ITA. The application used for this purpose is called “Dip on fiber” that allows to the TD-NMR device analyze the samples and return an electrical signal corresponding to the DPU. Then, it was necessary to do a linear regression between the DPU and this signal to obtain the calibration curve.

- **Validation of the TD-NMR curve**

Once the calibration curve is obtained, further validation is required. To validate the curve, 20 samples from the PD were measured in the TD-NMR device. The samples must be measured

three times, resulting in a total of 90 values to guarantee the feasibility of the curve. The results were compared with those obtained by PD quality control using the WCM. If the DPU values for the two methods have a lower difference than the maximum deviation implemented by the company, then the calibration curve will be implemented.

3.4 Study of mechanical properties - Bending stiffness test

The bending stiffness test evaluates the material's rigidity and is performed in equipment Zwick Z010 using the appropriate clamps. The procedure for this test is the following: ten cords are equally spaced out in the weaving comb, and three samples are marked with approximately 7 cm, avoiding the extremities of the comb. It is used tape to fix the cords, which are then cut. After the position of the clamps in the Zwick Z010 is adjusted, the sample is placed on the support of the upper sample holder, centered and parallel to the support frame. Finally, the test is initiated using the software interface.

The test requires three samples, and when placing the samples, it must be assured that the cords do not overlay; otherwise, the sample must be discarded. It is also important to avoid touching the surface of the samples or bending it to avoid interfering with their properties.

3.5 Statistical Analysis

To evaluate with accuracy the results obtained and decide whether the difference between the measured and standard value can be accounted for by random variations, significant statistical tests were performed. For that, Minitab 18 statistical software was used.

3.5.1 Significant tests

All the significance tests are based on the hypothesis test. The hypothesis test is a statistical method applied to statistical decisions through experimental data. It is essentially an assumption about the population parameter (any finite or infinite collection of individual units or objects). In these statistical tests, two statements are formulated: the null hypothesis (H_0) and the alternative hypothesis (H_1). The null hypothesis will be rejected in favor of the alternative hypothesis only if the sample evidence suggests that H_0 is false (Montgomery & Runger, 2003).

For the hypothesis test of the variances of two populations, each following a normal distribution, the null hypothesis states that the two variances are equal. In contrast, the alternative hypothesis states the opposite (Montgomery & Runger, 2003).

$$H_0 : \sigma_1^2 = \sigma_2^2 \quad (7)$$

$$H_1 : \sigma_1^2 \neq \sigma_2^2 \quad (8)$$

where σ_1^2 and σ_2^2 are the variances of populations 1 and 2, respectively.

For the hypothesis test of the means of two populations with equal variances that follow a normal distribution, the null hypothesis states that the means are equal, while the alternative hypothesis states the opposite (the means are not equal) (Gloriaful, 2022).

$$H_0 : \mu_1^2 = \mu_2^2 \quad (9)$$

$$H_1 : \mu_1^2 \neq \mu_2^2 \quad (10)$$

where μ_1^2 and μ_2^2 are the means of population 1 and 2, respectively.

To report the results of a hypothesis test, usually, a p-value approach is used, where the null hypothesis is accepted or rejected at a specified α-value or level of significance. The p-value is a measure of the strength of the evidence in the data against H_0. Usually, the smaller the p-value, the stronger the sample evidence is for rejecting H_0 (Montgomery & Runger, 2003).

3.5.2 Confidence Interval

Although hypothesis testing is a useful procedure sometimes does not provide all the information needed. Thus, it is used the confidence intervals which act as a reasonable estimate of the unknown parameters. A confidence interval (CI) estimates for a parameter θ an interval of the form $\mathrm{l} \leq \theta \leq \mathrm{u}$, where the endpoints are computed from the sample data. This CI is constructed based on probability theory, which mentions that there is a probability of $1 - \alpha$ of selecting a sample for which the CI will contain the actual value of the parameter θ (Montgomery & Runger, 2003).

$$H_0 : \theta = \theta_0 \quad (11)$$

$$H_1 : \theta \neq \theta_0 \quad (12)$$

There is a close relationship between the test of a hypothesis about any parameter θ and the CI for the same parameter. If (l, u) interval is the $100 \times (1 - \alpha)$ % CI for the parameter θ, the hypothesis test of size α will lead to the rejection of H_0 if and only if θ is not in the (l, u) interval (Montgomery & Runger, 2003).

4 Results and Discussion

The main goal of this dissertation was to obtain a calibration curve for Cokoon dipped Rayon for TD-NMR equipment to decrease the time spent on the standard method and improve the feasibility of DPU results. However, the composition of Cokoon dipped Rayon was developed recently. Hence, it was mandatory to study the reliability of the conventional method used for DPU determination, WCM, since a feasible method is needed to provide the reference values to calibrate the TD-NMR. To verify whether the WCM can be used for Cokoon dipping solution, a comparison was made between three different methods used to determine the DPU on dipped cords.

4.1 DPU Standard methods

4.1.1 Study of the Wet-Chemical Method for DPU determination

First, the Rayon greige cord was previously dissolved under WCM conditions to ensure that the solvents and experimental conditions used are ideal for the hydrolysis of Rayon fibers. To calculate the mass change of Rayon (Δm) that occurs during its dissolution, Equation 13 was used, where m_{i} is the initial mass of the greige cord, m_{c} is the mass of the crucible, and m_{f} is the mass of the crucible plus the residual cord after filtration.

$$\Delta m = \frac{(m_f - m_c) - m_i}{m_i} \times 100 \tag{13}$$

Table 5 shows the mean results for each fiber provided by supplier A and supplier B, the standard deviation (SD), and the associated coefficient of variation (CV). The results show that the experimental conditions used with this method are ideal for destructing these fibers since there was a mass loss of almost 100 %. This guarantee that in the trials with dipped cord, the fibber dissolves completely, remaining only the dip that was attached to the cord.

Table 5. Mass variation of Rayon fiber dissolved in formic acid with zinc chloride

Textile	Supplier	Mass Variation / %	SD / %	CV / %
Rayon	A	-99.61	0.09	0.09
Rayon	B	-99.70	0.25	0.25

After testing the reliability of this method for greige cords, a few trials were made for Rayon dipped with RFL and Cokoon. However, it was observed that for Cokoon dipped Rayon, after one hour of dissolution, there was still some suspension cord left undissolved, making vacuum filtration difficult. This may result from the fact that the two Rayon cords have a different linear density and are from a different supplier or even from the dipping solution. Thus, to optimize the method for the Cokoon, a study was conducted to determine the ideal dissolution

time. Six different times were tested, between 30 min and 120 min, and the DPU mean with the 95 % CI, calculated using the individual SD, are present in Figure 23. The results obtained are presented in Table A.2.1 of Appendix A.2.

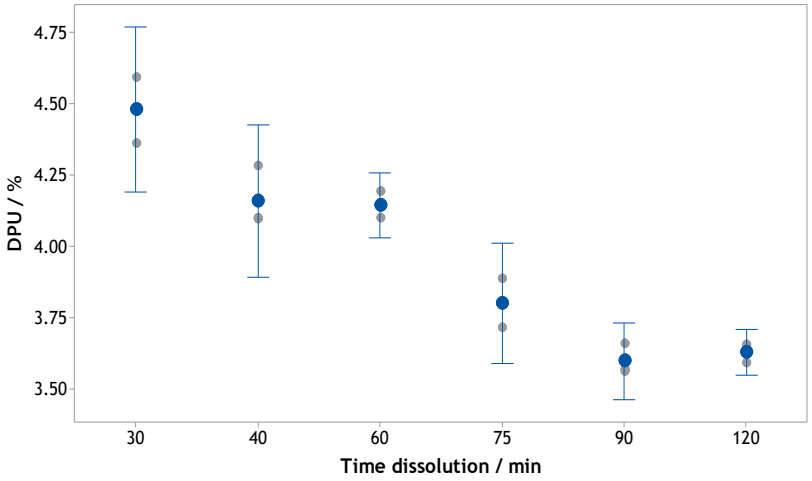

Figure 23. The influence of dissolution time on the DPU of Cokoon dipped Rayon with 95 % CI of the DPU mean and respective individual values.

The results indicate that until 90 min, increasing the dissolution time decreases the DPU values, probably due to the reduction of the undissolved suspension cord. However, between 40 and 60 minutes, the decrease in the mean DPU was not meaningful. Figure 24 shows the appearance of the residual solution during its washing on filtration, and it is possible to verify that for 30 minutes (Figure 24 a)), there is an undissolved cord, while for 90 minutes (Figure 24 b)), the washing fluids have no suspended fiber.

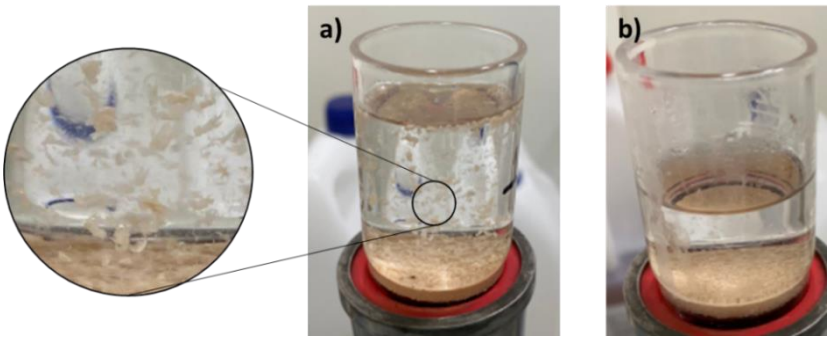

Figure 24. The appearance of the residual solution for 30 minutes of dissolution a) and for 90 minutes b).

Through Figure 23 and 24, it was possible to conclude that the ideal dissolution time for this Cokoon dipping solution is 90 minutes since the value of DPU remains after this time, and there are no undissolved fibers. Thus, the change in the Dip Pick-up value from 60 minutes to 90 minutes resulted in a decrease of the amount of dipping solution, with 95 % confidence bounds, from a $\mathrm{DPU}_{\text{per greige cord}} = 4.14 \pm 0.12$ % to $\mathrm{DPU}_{\text{per greige cord}} = 3.60 \pm 0.13$ %, respectively. After optimization of the dissolution time, several tests were performed for the same spool to

acquire repeatability and concordance in the results obtained with this method. The results of DPU are shown in Table 6. In addition, the same number of trials were made for the RFL dipping solution to prove that the way the operator performs the method is the same for the two dipping solutions. Appendix A.2 presents the results for each trial (Table A.2.2).

Table 6. DPU values for Cokoon and RFL dipped Rayon by Wet-Chemical Method

	RFL dipping solution			**Cokoon dipping solution**		
Cords	**Linear density = 2440 dtex**			**Linear density = 1840 dtex**		
	SC = 21.5 %			**SC = 7.7 %**		
Trials	**$DPU_{per\ greige\ cord}$ / %**	**SD / %**	**CV / %**	**$DPU_{per\ greige\ cord}$ / %**	**SD / %**	**CV / %**
1	6.79	0.08	1.15	3.61	0.03	0.93
2	7.14	0.01	0.16	3.67	0.07	1.86
3	7.14	0.08	1.13	3.61	0.01	0.41

It is possible to verify that the DPU values obtained for each trial are concordant with the conditions used for each Rayon fiber. The values obtained for the RFL dipped Rayon fit within the DPU target range specified for this material by the company. This proves that no errors occur in the performance of this method. After, the Weighing method was performed to compare the DPU values for each method, since for the standard RFL dipping solution, the results obtained by the two methods are approximately the same.

4.1.2 Weighing Method

For the WM, gloves were used in samples preparation to reduce the contact with the dip. The mean of DPU values obtained for each trial and the associated SD and CV are presented in Table 7.

Table 7. DPU values for RFL and Cokoon dipped Rayon by Weighing Method

	RFL dipping solution			**Cokoon dipping solution**		
Cords	**Linear density = 2440 dtex**			**Linear density = 1840 dtex**		
	SC = 21.5 %			**SC = 7.7 %**		
Trials	**$DPU_{per\ greige\ cord}$ / %**	**SD / %**	**CV / %**	**$DPU_{per\ greige\ cord}$ / %**	**SD / %**	**CV / %**
1	7.46	0.33	4.44	5.23	0.15	2.89
2	7.34	0.28	3.77	5.53	0.18	3.21
3	7.22	0.29	4.02	5.42	0.28	5.21

As expected, the RFL dipping solution results show that the DPU obtained by WCM and WM are very similar. Therefore, the two methods can be used to determine dip content of RFL on Rayon dipped cords. However, the same was not valid for the Cokoon dipping solution, as the DPU results are significantly higher for WM. This might occur due to a loss of components of Cokoon dipping solution during the procedure of WCM. Two mechanisms justify the mass loss in this formulation during WCM performance. One is related to some free substances that do not react with the fiber, such as ε-caprolactam, which, after the MDI isocyanate deblocking reaction, is released and, according to Rolph et al. (2016), does not volatilize. Furthermore, caprolactam is soluble in water and chlorinated solvents and has a melting point of 70 °C, which is the dissolution temperature used in WCM (Information, 2022). Thus, after dissolution, this blocking agent is already solubilized, being eliminated along with the washing fluids during filtration, which accounts for the weight loss. The other way to lose mass in Cokoon dip residue is the possibility of loss of dip components, which after reacting with the solvents used, may be solubilized or are released to the atmosphere as gases.

Since the results obtained for the two methods were not concordant, another chemical method was tried to compare the DPU values.

4.1.3 Kordsa-Chemical Method

Kordsa company provided its chemical method for determining DPU values, allowing comparison with the results obtained by WCM and WM, used in the C-ITA. The principle of the method is very similar to the WCM, with the main difference being the solvent used, sulfuric acid. However, some adjustments had to be made, as the procedure provided was not detailed by the company. Regarding the dissolution time, three different times were tested, as shown in Table 8.

Table 8. Influence of the time dissolution in the DPU values of Cokoon dipped Rayon, through the Kordsa-Chemical Method

Time	DPU / %	SD / %	CV / %
60	5.47	0.18	3.32
90	4.80	0.08	1.57
120	4.58	0.09	1.95

The results showed that lower values of DPU were obtained with increasing dissolution time as in WCM; however, a longer dissolution time is required for this method. Furthermore, after filtration, it appears that the fibers do not completely dissolve, and although increasing dissolution time increases their hydrolysis, a residue without undissolved cords was never obtained. Figure 25 shows the appearance of the filtration residue (dip) for the three different

times tried. Thus, the selected dissolution time was 120 min since, according to Figure 25, it corresponds to the crucible containing, apparently, less undissolved fiber.

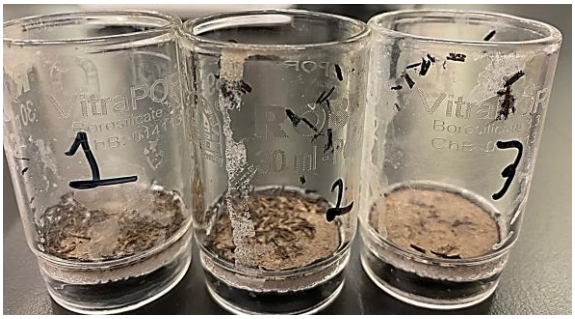

Figure 25. Result of filtrating the Cokoon dipped Rayon, dissolved for 60 minutes (l1), 90 minutes (2), and 120 minutes (3).

After optimization of the dissolution time, three trials were performed for two hours of dissolution and a water bath temperature of 40 ºC. The results are presented in Table 9.

Table 9. DPU values for RFL and Cokoon dipped Rayon by Kordsa-Chemical Method

	RFL dipping solution			**Cokoon dipping solution**		
Cords	**Linear density = 2440 dtex**			**Linear density = 1840 dtex**		
	SC = 21.5 %			**SC = 7.7 %**		
Trials	**DPU / %**	**SD / %**	**CV / %**	**DPU / %**	**SD / %**	**CV / %**
1	8.10	0.30	3.68	4.52	0.31	6.94
2	7.82	0.33	4.21	4.49	0.17	3.85
3	8.31	0.13	1.53	4.58	0.09	1.95

Comparing the standard deviations and the coefficients of variation obtained using the WCM (Table 6) with those obtained by KCM (Table 9) it is clear that for the latter, there is a more significant variation in the DPU results for the three replicates performed for each trial.

The higher values of DPU obtained for RFL compared to the WCM can be justified by possible reactions between the latex components and sulfuric acid since electrophilic addition reactions between sulfuric acid and alkenes usually occur to produce alkyl hydrogen sulphates (Clark, 2020). Thus, the VP-latex, the Styrene-Butadiene Rubber (SBR-Latex) and the natural rubber, present in the composition of RFL dipping solutions, can react with the sulfuric acid producing alkyl hydrogen sulphates just like ethene reacts to give ethyl hydrogen sulphate (Equation 14) (Clark, 2020). The alkyl hydrogen sulphates will result in an increase in the mass. Besides Cokoon dipping solution contains the same latexes as RFL dipping solution, in the case of the new formulation, the loss of free components such as caprolactam may be greater than the gain of mass from the reaction with latex.

$$RCH = CHR + H_2SO_4 \rightarrow RCH_2CH(OSO_2OH)R \quad (14)$$

In addition, the MDI isocyanate after deblocking reaction acquires its functional reactivity and according to Liessem (1983) and Ionescu (2019), possible reactions can occur between isocyanates and formic acid to liberate gases like carbon dioxide and carbon monoxide gases (Figure 26), also justifying the decrease of mass. During the dissolution step of WCM, about 1 mol of formic acid generates 2 mol of gases: 1 mol of carbon dioxide and 1 mol of carbon monoxide, contributing to a decrease in the mass fraction associated to the MDI (Ionescu, 2019).

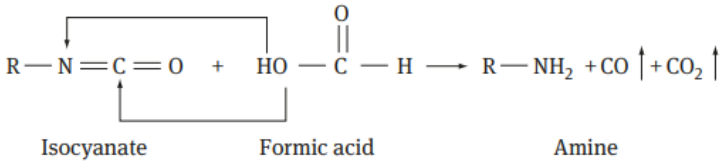

Figure 26. Reaction of an isocyanate group with formic acid (Ionescu, 2019).

4.1.4 Comparison of DPU values obtained by the different methods

To understand which is the best method to determine the DPU of the Cokoon dipped Rayon, the values obtained with the three methods, presented in Table 6, 8, and 10, were compared with a 95 % confidence interval (Figure 27).

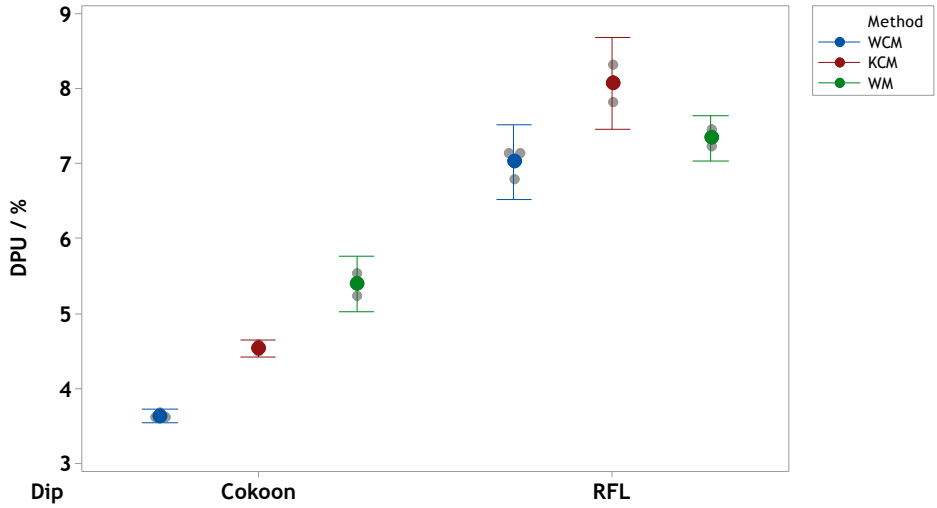

Figure 27. DPU measurements for RFL and Cokoon dipping solutions with 95 % CI for WCM, KCM, and WM.

The DPU values obtained by each method should be similar for each dipping solution, meaning that the DPU mean value is not affected by the method of determination applied. However, analyzing the graph in Figure 27, it is clear that this does not happen. The one-way ANOVA procedure was used to test if the different methods do not affect the mean DPU values for each dipping solution, RFL and Cokoon. However, first, the variances of DPU values of the three methods were tested for each dipping solution to check if they were different and, in both

cases, it was concluded that there is no statistical evidence that they are different since the p-value was larger than 0.05 for the two cases (Figure A.2.1 and Figure A.2.2 of the Appendix A.2). The one-way ANOVA procedure, assuming equal methods' DPU variances, is summarized in Table A.2.3 and Table A.2.4 from Appendix A.2. Since the p-value obtained was 1.392×10^{-6} for Cokoon dip and 1.586×10^{-3} for RFL dip, much inferior to 0.05, it was concluded that the methods affect the mean DPU values for each dipping solution.

Tukey's method was applied to determine which DPU means are statistically different for each dipping solution and the results are presented in Table 10 and Table 11. Regarding the RFL, through Table 10, it could be affirmed that the WM and WCM DPU means are not statistically different (p-value = 0.1991 > 0.05) and that KCM and WCM DPU means and WM and KCM DPU means are statistically different (p-value = 1.456×10^{-3} << 0.05 and p-value = 8.844×10^{-3} << 0.05, respectively).

Table 10. Tukey tests for differences of means in DPU methods for RFL dipped Rayon

	Difference of means / %	**SE / %**	**95 % CI**	**p-value**
KCM – WCM	1.053	0.160	(0.561, 1.545)	1.456×10^{-3}
WM – WCM	0.317	0.160	(-0.175, 0.809)	0.1991
WM – KCM	-0.737	0.160	(-1.229, -0.245)	8.844×10^{-3}

Relatively to the Cokoon, it could be verified that all pairs of DPU means are statistically different since the p-values are all inferior to 0.05 (Table 11). Thus, it was decided to choose one of the three methods studied based on their comparison in order to have a feasible method to provide the DPU reference values to the TD-NMR. The WM is the only one that does not involve interference with the dipping solution since it does not use hazardous solvents to destroy the cords and, besides that, were used gloves during the preparation of the samples to reduce the possibility of introduction of components by the operator's hand into the cord. Therefore, it was decided that the WM is the most reliable for determining the DPU of Cokoon dipped Rayon.

Table 11. Tukey tests for differences of means in DPU methods for Cokoon dipped Rayon

	Difference of means / %	**SE / %**	**95 % CI**	**p-value**
KCM – WCM	0.9000	0.0765	(0.6652, 1.1348)	6.341×10^{-5}
WM – WCM	1.7633	0.0765	(1.5286, 1.9981)	1.041×10^{-5}
WM - KCM	0.8633	0.0765	(0.6286, 1.0981)	7.851×10^{-5}

4.2 TD-NMR Calibration Curve

The focus for comparing the methods mentioned was to get a reliable one that can be used as a reference to obtain a calibration curve for Cokoon dipped Rayon with TD-NMR. It was concluded that WM is the best one to use with this material. However, to validate a calibration curve, it is necessary to perform the same method used to calibrate the TD-NMR. Nevertheless, the samples kept so far do not have the length (100 meters) needed to perform this method. Furthermore, the same quantity of thermofixed cord is needed, and this is not produced on the Zell machine since the method used in PD until now for this material was the WCM. So, it would be necessary to use the LDU to thermofix the Rayon, which would result in a larger associated error because the same machine would not be used to obtain the dipped fabric and thermofixed fabric, potentially influencing the material properties. Therefore, it was mandatory to find a way to validate the curve obtained by this method. Through the comparison of the methods, it was noticed that the difference of the DPU means, with 95 % confidence bounds, for WCM and WM was about 1.76 ± 0.23 % for the same formulation. So, it was necessary to understand if this difference is constant for all Cokoon formulations. Therefore, the two methods were applied to the four cords with different DPU values needed to perform the calibration curve. If the difference is systematic, a correlation can be made between the DPU values obtained by the two methods, allowing to calculate the DPU for the WM through the DPU value obtained by the WCM.

The four cords (A, B, C and D) were obtained using Cokoon dipping solutions with different SC in the LDU. However, it was necessary to perform the WCM to achieve the required DPU in the range stated in Table 12 for each cord. The WCM was used because the DPU tolerance range implemented by the company to Cokoon dipped Rayon was specified based on this method, and the values of LTL, T, and UTL are mentioned in section 4.5.1. The DPU results for each method and the variation between them, DPU_{WM}-DPU_{WCM}, are presented in Table 12. The DPU_{WM} and DPU_{WCM} correspond to the DPU results obtained by the WM and WCM, respectively. The values of each trial are attached in Appendix A.3, Table A.3.1 and Table A.3.2.

Table 12. Rayon samples used for calibration with DPU measurements by WCM and WM

Cord	DPU Range / %	DPU_{WCM} / %	SD_{WCM} / %	DPU_{WM} / %	SD_{WM} / %	DPU_{WM}-DPU_{WCM} / %
A	1 - 2	1.56	0.03	2.95	0.05	1.39
B	2 – 3.5	3.21	0.08	5.51	0.09	2.30
C	3.5 – 5	4.85	0.04	7.09	0.12	2.24
D	5 - 6	5.62	0.05	7.78	0.16	2.16

The difference between the DPU values for the two methods remains at approximately 2 % for cords B, C and D. However, a smaller difference is noted for the cord with lower Solid Content. This can be explained by the fact that 95.3 % of the Cokoon dipping solution for cord A is water, which means that there is a meager amount of solids to react with the solvents used in the dissolution, resulting in a lower loss of dipping solution. For example, not all the hydroxy groups in Rayon cords may react with the dipping solution components resulting in more straightforward hydrolysis of the fibers.

In order to obtain a correlation between the DPU values obtained with the two methods, it was necessary to perform two calibration curves: one using the WCM as a reference and the other using the WM.

- **TD-NMR calibration curves**

The two calibration curves obtained with TD-NMR equipment with 95 % CI and 95 % Prediction Interval are presented in Figure 28 and will be referred to WCM_{curve} for the one obtained using the WCM and WM_{curve} for the other obtained by WM. The reference values of DPU and the signal provided by TD-NMR for the WCM_{curve} and WM_{curve} are presented in Appendix A.3, Table A.3.3 and Table A.3.4, respectively.

In order to check the fit of the calibration curve to the experimental data, the assumption that the model is linear and that the errors follow a normal distribution with zero mean and constant variance should be validated through the analysis of the residual plots of the WM_{curve} and WCM_{curve}, (Figure 29 and Figure 30). Residual is the difference between the observed and the predicted value.

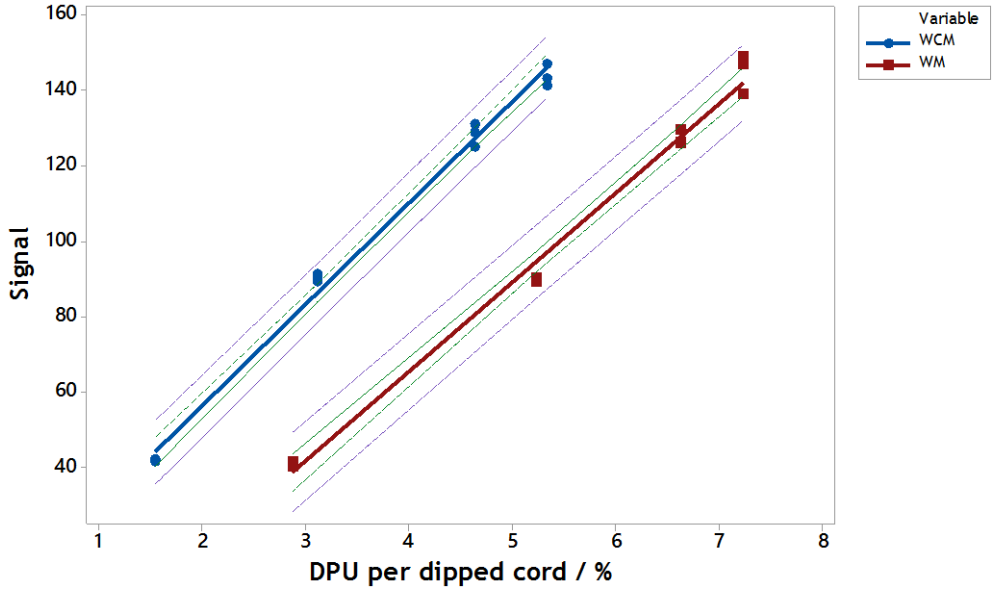

Figure 28. TD-NMR calibration curves for Cokoon dipped Rayon using the WCM and WM.

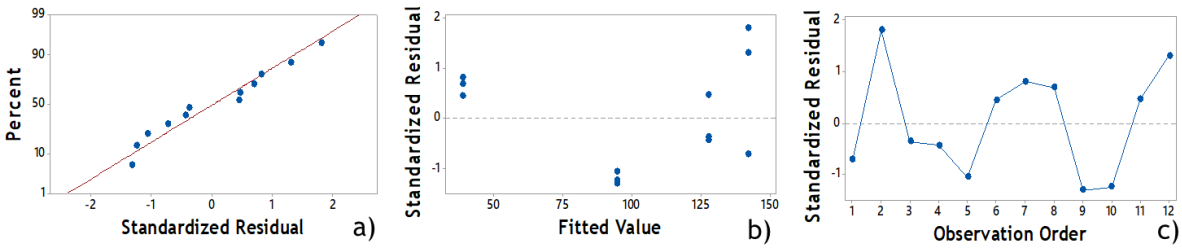

Figure 29. Residual plots for WM_{curve}: a) Normal Probability Plot; b) Versus Fits; c) Versus Order.

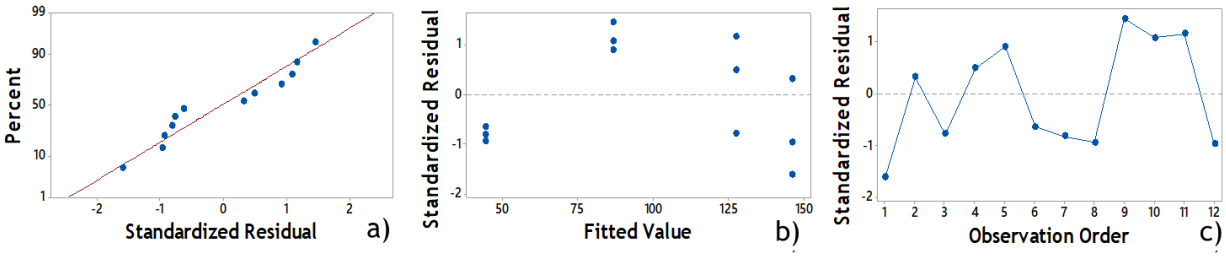

Figure 30. Residual plots for WCM_{curve}: a) Normal Probability Plot; b) Versus Fits; c) Versus Order.

Analyzing the normal probability plot for the two curves, (Figure 29 a) and Figure 30 a)), the residuals appear to follow an approximately normal distribution since the values seem to follow a linear shape. Thus, it can be concluded that there are no significant deviations from the normality of the random errors. Observing the residuals versus fitted values plots (Figure 29 b) and Figure 30 b)), the values are randomly distributed around the zero line, suggesting that the equal variance assumption is followed. Furthermore, in the residual versus observation order plots (Figure 29 c) and Figure 30 c)), a random distribution around the centerline can be seen, demonstrating that the values seem to be independent. This proves that the calibration curves fit the experimental data. Then, the key results for the fit regression model were analyzed for the two curves: the SE, the 95 % CI, and the p-value for each model coefficient (Table 13).

Table 13. Regression coefficients for the WCM_{curve} and WM_{curve} and respective statistical characteristics

		Coefficient	SE	95 % CI	p-Value
WCM_{curve}	Slope	26.92	0.66	(25.45, 28.39)	1.89×10^{-12}
	Intercept	2.70	2.60	(-3.08, 8.48)	3.20×10^{-1}
WM_{curve}	Slope	23.70	0.72	(22.10, 25.31)	3.35×10^{-5}
	Intercept	-29.29	4.13	(-38.50, -20.08)	1.60×10^{-11}

The confidence interval of the slope is minimal for the two curves, meaning that the slope estimate is very close to 26.92 for the WCM_{curve} and 23.70 for the WM_{curve}. Besides that, the p-value is much lower than 0.05, meaning there is a statistically significant association between the TD-NMR signal and the DPU reference values. The 95 % confidence error margin of the

intercept of the WCM_{curve} is lower than the one of the WM_{curve}. The WCM_{curve} and WM_{curve} are characterized, with 95 % confidence bounds, by the mathematical expressions shown in Equations 15 and 16, respectively.

$$\text{Signal} = (2.70 \pm 5.78) + (26.92 \pm 1.47)\ \text{DPU}_{\text{per dipped cord}} \tag{15}$$

$$\text{Signal} = (-29.29 \pm 9.21) + (23.70 \pm 1.60)\ \text{DPU}_{\text{per dipped cord}} \tag{16}$$

To assess the quality of the linear regression fitting, two variables can be studied: SE and the determination coefficient (R^2). The SE represents the mean distance the observed values fall from the regression line. A lower value of SE corresponds to the closer proximity of the observed values to the fitted line. The R^2 value provides the proportion of the dependent variable variation that the model explains and usually is expressed in percentage; according to C-ITA standards, this value must be higher than 90 % to consider a suitable calibration. The results for these parameters are presented in Table 14, and it is possible to conclude that the two curves have a determination coefficient higher than the one specified by the company. Therefore, the calibration curves fit the experimental data, following the company criteria.

Table 14. Linear regression statistical measures for the Cokoon dipped Rayon's calibration curves

	R^2 / %	SE / %
WCM_{curve}	99.4	3.33
WM_{curve}	99.1	4.18

Since the two curves appear to follow a good linear regression and seem parallel, it was induced that it is possible to make a correlation between them.

4.2.1 Correlation between the WCM and WM

The correlation obtained between the WCM and WM is presented in Figure 31.

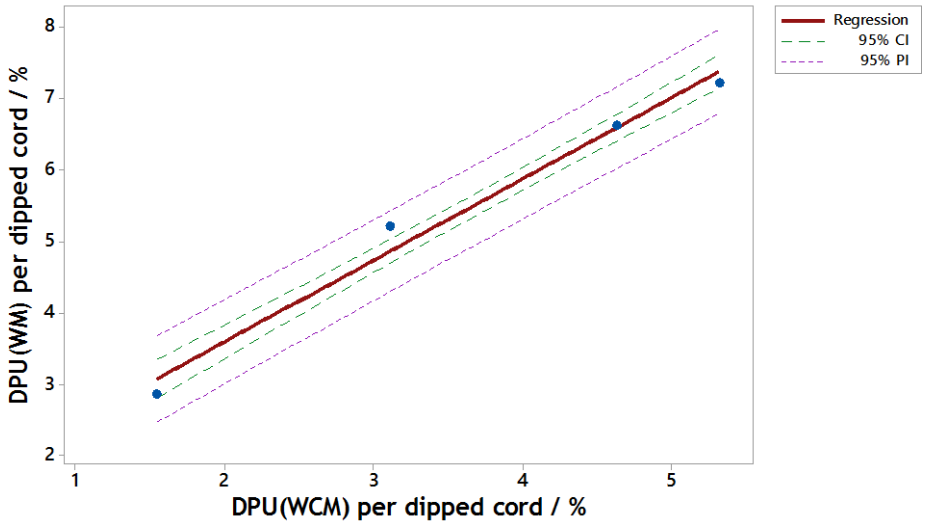

Figure 31. Regression curve to correlate the DPU_{WCM} with the DPU_{WM}.

The values of DPU obtained by the two methods appear to follow a linear regression. However, residual plots were created to confirm the linear regression model and can be found in Appendix A.3 (Figure A.3.1). Analyzing those plots makes it possible to verify that the data checks out all linear regression model assumptions. So, it is considered that the DPU results of each method follow that model.

The regression equation for this correlation is given by Equation 17, where DPU_{WCM} corresponds to the DPU values obtained by WCM and $\mathrm{DPU_{WM}}$ to the ones obtained with the WM.

$$\mathrm{DPU_{WM}} = 1.326 + 1.139\ \mathrm{DPU_{WCM}} \tag{17}$$

The R^2 value is relatively high, 98.25 %, so higher than 90 %, and the value of SE obtained was 0.2422. So, it can be concluded that the linear regression model for the correlation provides a good fit.

4.2.2 Validation of the calibration curve

The WM_{curve} had to be validated to verify if it could measure the amount of DPU from production samples. However, the Cokoon dipped Rayon was only produced twice this year in the PD, so only two recent samples could be collected. Usually, samples are only kept for six months since external parameters can affect their properties after this period. However, there are no studies that prove this claim. Therefore, besides the two samples collected from this year, samples from 2020 and 2021 were also used, which have been stored in the Laboratory since then. For the validation of the WM_{curve} the scheme in Figure 32 was followed. Twenty Cokoon dipped Rayon samples were used and the DPU values provided by TD-NMR ($DPU_{TD\text{-}NMR}$), and the Weighing Method for these samples should be compared. To obtain the values for the WM, it is necessary to calculate the DPU value using the WCM. Besides Production Department already determining these values with this method, the procedure was repeated for all samples with the optimized dissolution time, i.e., with 90 min instead of 60 min. The results are present in the Appendix A.3 (Table A.3.5). Considering that TD-NMR gives DPU values per dipped cord and the WCM and WM per greige cord, the Equation 6 was used to convert the DPU values and work in the same units. Thus, the DPU of the 20 samples was measured by TD-NMR and WCM. The values provided by WCM were converted to WM through the correlation (Equation 17) and compared with the DPU values from TD-NMR.

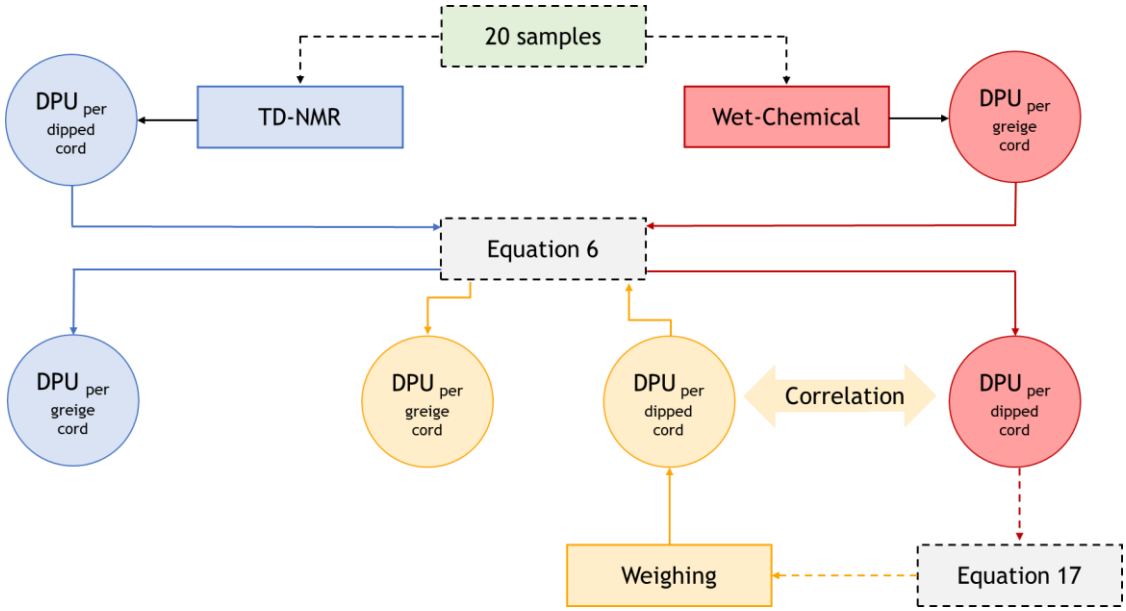

Figure 32. Scheme of the validation step for the WM_{curve}.

The comparison between the results of the WM and TD-NMR measurements is shown in Figure 33. The x-axis represents the samples used and the corresponding storage time in months. In addition, the DPU target range values for this material with this method are present in the graph as T, LTL, and UTL. However, these values were also calculated using the correlation since it does not make sense to use the values specified for the WCM. Thus, instead of a T of 3.5 %, an LTL of 2 %, and a UTL of 5 %, it becomes 5.3 %, 3.6 %, and 7 %, respectively. The DPU values obtained for each method are present in Table A.3.6, Appendix A.3.

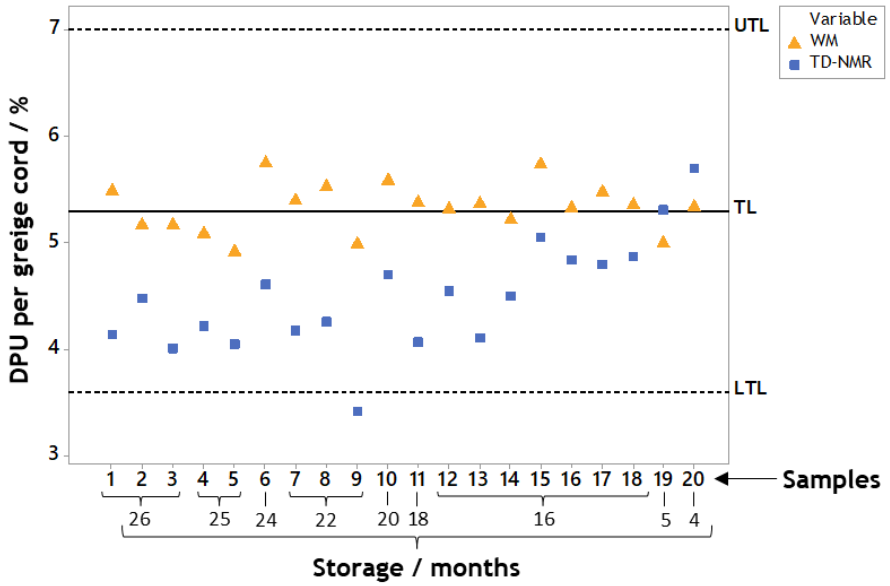

Figure 33. Validation of the calibration curve using Cokoon dipped Rayon samples with different storage time: comparison between the TD-NMR measure and the WM values.

According to the protocol of C-ITA, the approval criterion for the material is an absolute maximum deviation between the results of the two methods, $|DPU_{WM} - DPU_{TD\text{-}NMR}|$, of 0.563.

Considering the DPU values achieved in Figure 33, it can be concluded that a considerable difference between the two methods is noticeable for the older samples. The $DPU_{TD\text{-}NMR}$ values tend to be considerably lower, except for the two recent samples. For the samples collected from this year, 19 and 20, the measurements of DPU by the two different methods were approximately concordant, meeting the maximum deviation requirement, $|DPU_{WM} - DPU_{TD\text{-}NMR}| \leq 0.563$. In addition to these two samples, sample number 16 also meets the requirement; however, unlike samples number 19 and 20, the $DPU_{TD\text{-}NMR}$ result was lower than that of the DPU_{WM}. Usually, the DPU obtained by this device is higher than that obtained by standard methods, which induces that the problem in this validation is related to the age of the samples.

To study the reliability and confidence of the results obtained through statistical analysis, a two-sample t-test was made to verify the equality of the DPU means. However, to select the appropriate test, it is necessary to confirm if the variances are equal. So, a variance test was done for any continuous distribution, and the results of the equal variances test can be seen in Table A.3.7 and Figure A.3.2, Appendix A.3. It is possible to conclude that the variances of the DPU values for the TD-NMR and WM methods differ significantly since the p-value obtained was lower than 0.05 for Bonnet and Levene methods.

Afterward, a two-sample t-test was performed to test the equality of the DPU means of both methods, assuming different DPU variances. The test results are shown in Table 15, and the boxplot representation of the DPU values with the sample mean for both methods is present in Appendix A.3 in Figure A.3.3. Since the p-value (5.31×10^{-6}) obtained was much lower than 0.05, it was concluded that the DPU means of the methods are different.

Table 15. Two sample t-test results for the comparison of WM and TD-NMR

	DPU Mean / %	SD / %	Means difference / %	95 % CI	p-Value
TD-NMR	4.485	0.518	-0.839	(-1.100, -0.578)	5.31×10^{-6}
WM	5.323	0.233			

The means of the DPU determined by WM and TD-NMR have an estimated difference of 0.84 ± 0.27 %, which is higher in absolute value than 0.563, so it was concluded that the calibration curve developed did not meet the criterium for approval. However, the validation step for the WM_{curve} can be repeated in the future with samples with less than six months of storage since the criterium was not achieved only for the samples with more than this storage time.

4.3 Study of mechanical properties

To evaluate if the age of the samples influences the mechanical properties, a study was made. The 20 samples used to validate the WM_{curve} did not have enough material to perform all mechanical tests, so the stiffness test was conducted. This property had special attention

because, in the preparation of the samples, it was noted that, in the older ones, more precisely from 2020 and 2021, the fabrics have different behavior, appearing to be stiffer. The results of the stiffness values with 95 % CI for each sample are presented in Figure 34; however, samples 6 and 15 do not have sufficient amount of cord to perform the test. Globally, the samples with less storage time have lower values of stiffness, which induces an increase in this property with the increase of the storage time. Comparing the behavior of this mechanical property with the one for DPU provided by TD-NMR (Figure 35), it is possible to conclude that they have opposite trends.

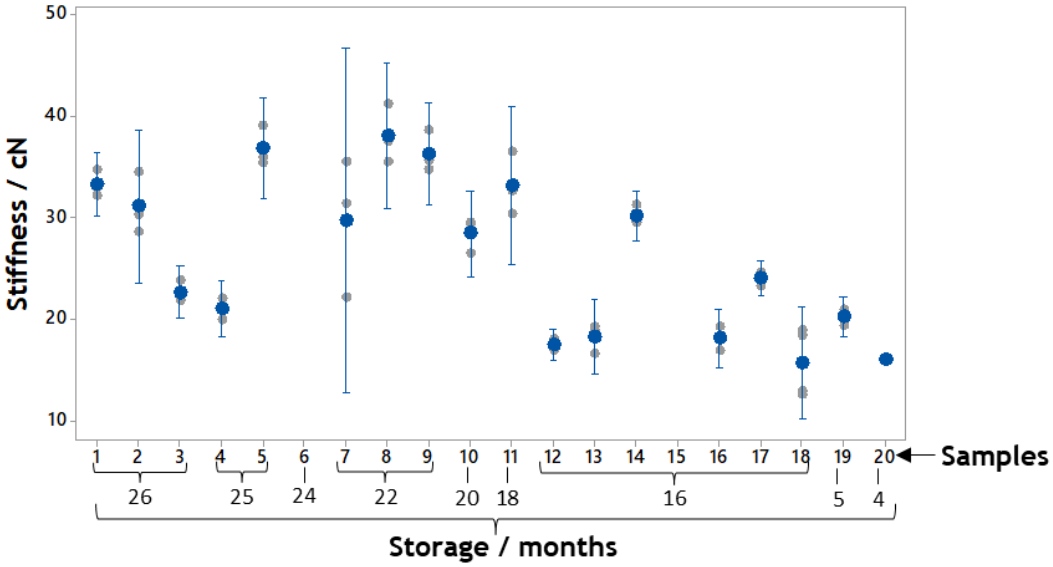

Figure 34. Results of the Bending Stiffness study with 95 % CI for twenty samples of Cokoon dipped Rayon with different storage time.

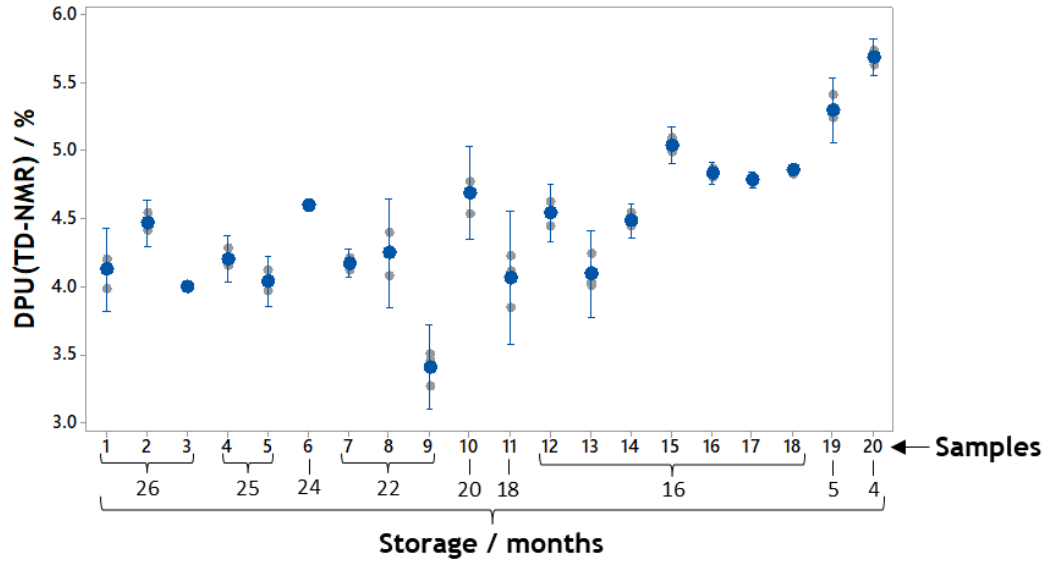

Figure 35. Results of the DPU provided by TD-NMR with 95 % CI for twenty samples of Cokoon dipped Rayon with different storage time.

Analyzing the two figures (Figure 34 and Figure 35), it is possible to conclude that the stiffness of the samples may influence the TD-NMR analysis since the lower DPU values were obtained with the stiffer samples. This can be related to the molecular motion in the dip attached to the cord that influences the relaxation time T1 in TD-NMR. The samples with higher stiffness values have lower vibrational and rotational energies associated with the lower motional states of the atoms in the surrounding environment. Thus, the necessary energy exchange between the spin system and the environment may not be sufficient, affecting the longitudinal relaxation and resulting in lower DPU values.

5 Conclusion

The purpose of this master's dissertation was to calibrate the TD-NMR equipment for Cokoon dipped Rayon allowing the progress of quality control in C-ITA. However, the Cokoon dip solution was developed recently, so before it was needed to evaluate the reliability of the standard method, the Wet-Chemical Method, used in the company for Rayon.

In the first part of this project, the Wet-Chemical Method and the Kordsa-Chemical Method were optimized regarding the dissolution time used for Cokoon dipped Rayon since, during one hour of dissolution, there was still some suspension cord left undissolved. It was concluded that 90 minutes of dissolution time is required for WCM and 120 minutes for KCM. The Dip Pick-up results for these two optimized chemical methods were compared with each other and with a third method, the Weighing Method, which does not use chemicals to determine the dip content. The results were not concordant, and it was noticed that the Weighing Method provided the highest DPU values, 1.76 ± 0.23 % higher than WCM and 0.86 ± 0.23 % higher than KCM. The same comparison was made for Rayon dipped in RFL, and the same behavior was not observed since the two methods used in C-ITA, WCM, and WM gave similar DPU results, as expected. Thus, it was concluded that during the WCM and KCM procedure, a loss of components from the Cokoon dipping solution probably occurs due to the elimination of free components such as caprolactam during the filtration step and released gases resulting from possible reactions. The Weighing Method was suggested as an alternative to the Wet-Chemical Method for determining the dip content in Cokoon-treated Rayon fibers since it is a non-destructive method. Such results are crucial for C-ITA, as it shows that the method used so far to determine the Dip Pick-up material for Rayon cannot be used for the dip composition of Cokoon. Thus, the DPU Target Range should be adjusted according to the results provided by WM.

In the second part of the project, the TD-NMR device was successfully calibrated for Cokoon dipped Rayon with the DPU results of the Weighing Method. However, to validate the curve with the WM, a correlation between the DPU results obtained by WCM and WM was needed since in Production Department it was not produced thermofixed fabric Rayon to perform the procedure of this method. Thus, to validate the curve, the WCM was performed, and the DPU results were converted to DPU corresponding to the WM. The validation was carried out with 20 samples, and the results did not allow its implementation since it was shown that the means of both populations, $DPU_{TD\text{-}NMR}$ and DPU_{WM}, had an estimated difference of 0.84 ± 0.27 % in absolute value, superior to the criteria established for the material, 0.563. However, the results lead us to believe that the age of the samples influences the TD-NMR measurements since only

the samples with more than six months of storage presented lower values of the DPU measured in this device.

The final part of this dissertation conducted a study of the stiffness of the 20 samples of Cokoon dipped Rayon from 2020 to 2022. The results showed that the stiffness value was higher for almost all samples older than six months, corresponding to a lower DPU value in TD-NMR. This proves that the TD-NMR analysis is influenced by the mechanical properties of the materials, like the stiffness of the samples, which in turn can be affected by external parameters over time.

The last two parts of the project allowed C-ITA to have more details about TD-NMR since no studies had been carried out until now based on the influence of mechanical properties on the DPU measured by this equipment. Besides that, the correlation between WCM and WM allows the company to determine the DPU values with WM without performing it, i.e., continuing to use the conventional method that when substituted in the correlation gives the DPU values corresponding to the Weighing Method.

6 Assessment of the work done

6.1 Objectives Achieved

This dissertation aimed to study the Wet-Chemical Method's reliability and calibrate the TD-NMR device to allow its use for Cokoon dipped Rayon.

According to the studies made for the chemical method used in C-ITA, it was concluded that it is unreliable when applied to Cokoon dipping solution in the case of Rayon material.

Relatively to the TD-NMR, two calibration curves were obtained, one with the Wet-Chemical Method and the other with the WM. However, neither one was approved due to the scarcity of samples produced in the PD this year.

6.2 Other Work Carried Out

The company proposed to add a new point to an existing TD-NMR calibration curve for nylon fabric, with a linear density of the cord of 940 dtex, whose raw material is supplied by C. However, C-ITA has a new supplier, D, who supplies the nylon yarn to produce nylon dipped cord, with the same linear density as nylon C. However, the DPU values obtained so far for the nylon dipped cord are higher than the UTL of the range specified for nylon fabric C. Thus, it was necessary to add a new point to the calibration curve in order to be able to measure the DPU for the new material with the TD-NMR. Different samples were obtained in the LDU with a more concentrated dipping solution, i.e. with a higher DPU. Since the nylon from the older supplier was not currently produced in the company it was necessary to twist the nylon yarns using the Laboratory Twisting Unit. After adding the new point to the calibration curve, it was necessary to validate it with 15 samples from production. However, the TD-NMR measurements provided significantly higher DPU values than the WCM, suggesting that the nylon supplied by D needs its own calibration curve. This might occur because the conditions used in PDU are different for the two materials and besides that, the nylon C is produced in the Zell machine and nylon D in the Single-end machine.

6.3 Limitations and Future Work

Regarding limitations, the main difficulty was, without a doubt, the time available. The WCM takes about 4 hours per sample, and although it was possible to make more than one Dip Pick-up simultaneously, the laboratory must be shared with the other workers.

In the future, it would be interesting to continue the validation step to the WM_{curve} when the Cokoon dipped Rayon samples are available in the PD, excluding the older samples.

In addition, it would be advantageous to do a more in-depth study of the parameters involved in TD-NMR equipment like the default scans number, the recycle delay RD and the sampling time since the definition of these parameters was never adjusted for this new dipping solution. Besides that, it is also important to understand if the mechanical properties of the material influence the DPU measurements on the TD-NMR equipment.

It also would be interesting to perform an analysis of the natural aging of Cokoon dipped Rayon to study the stability of its mechanical and chemical properties. For that, a high number of samples need to be kept in bag conditioning over two or three years, and every month the same chemical and mechanical tests should be performed in order to see if the properties of this material are affected by storage time.

Regarding to the WCM, a different isocyanate should be tried in Cokoon dipping solution and verify if the DPU values obtained with this method increase. If that happens, probably the loss of mass can be justified by the assumptions made in section 4.1.3.

6.4 Final Assessment

I am forever grateful to C-ITA for this incredible learning experience. I am proud of the work that I developed. It was not always straightforward; there were numerous difficulties and obstacles. However, with my co-workers' help and good ambiance, everything became easier to overcome. I hope that in the future, the curves obtained for this material can be validated with recent samples and contribute to improving the quality control of C-ITA.

7 References

- Aubin, Y., Keire, D. A., Marino, J. P., & Freedberg, D. L. Chapter 13 - One- and two-dimensional NMR techniques∗. In D. J. Houde & S. A. Berkowitz (Eds.), *Biophysical Characterization of Proteins in Developing Biopharmaceuticals* (pp. 375-430). United States: Elsevier, 2020.
- Avar, G., Meier-Westhues, U., Casselmann, H., & Achten, D. 10.24 – Polyurethanes. In K. Matyjaszewski & M. Möller (Eds.), *Polymer Science: A Comprehensive Reference* (pp. 411-441). Amsterdam: Elsevier, 2012.
- Bainbridge, A. Nuclear Magnetic Resonance Spectroscopy | Overview. In P. Worsfold, A. Townshend, & C. Poole (Eds.), *Encyclopedia of Analytical Science (Second Edition)* (pp. 203-211). Oxford: Elsevier, 2005.
- Besghini, D., Mauri, M., & Simonutti, R. Time Domain NMR in Polymer Science: From the Laboratory to the Industry. Italy: *Applied Sciences, 9*(9). (2019). Retrieved from (https://doi.org/10.3390/app9091801).
- Bilisik, K. Multiaxis Three Dimensional (3D) Woven Fabric. In Advances in Modern Woven Fabrics Technology (Ed.), 2011.
- Britannica, E. o. E. Tire. In *Encyclopedia Britannica, 2016*.
- Britannica, E. o. E. Solution. In *Encyclopedia Britannica, 2019*.
- Bruker. *Time-Domain NMR: Basic Principles and Real-World Applications Printable Document*. (2015). Retrieved March 11, 2022 from (https://www.news-medical.net/webinar/Time-Domain-NMR-Basic-Principles-and-Real-World-Applications).
- Burak Erman, J. E. M. a. C. M. R. *The Science and Technology of Rubber* (Fourth Edition ed.). United States of America: Elsevier B.V, 2013.
- Cao, N., Xu, Q., & Chen, L. Acid hydrolysis of cellulose in zinc chloride solution. *Applied Biochemistry and Biotechnology, 51*(1), 21-28, 1995.
- Clark, J. Reactions of Alkenes with Sulfuric Acid. (2020) Retrieved June 25, 2022 from (https://chem.libretexts.org/Bookshelves/Organic_Chemistry/Supplemental_Modules_(Organic_Chemistry)/Reactions/Addition_Reactions/Electrophilic_Addition_Reactions/Reactions_of_Alkenes_with_Sulfuric_Acid).
- Continental. Tyre Basics Passenger Car Tyres. (2013 / 2014). Retrieved from (https://kipdf.com/tyre-basics-passenger-car-tyres_5ad49b767f8b9adb308b45e3.html).
- Continental. Factos & Números. (2015a). Retrieved March 6, 2022 from (https://www.continental-pneus.pt/ligeiros/empresa/sobre-n%C3%B3s/corporativo).
- Continental. Produção de pneus. (2015b). Retrieved March 6, 2022 from (https://www.continental-pneus.pt/ligeiros/conhecimento-pt/fundamentos-dos-pneus/producao-de-pneus).
- Continental. German Workmanship Values Lived Globally. (2022a). Retrieved March 6, 2022 from (https://www.continental-tires.com/car/why-continental/german-engineering).
- Continental. Tire components. (2022b). Retrieved March 6, 2022 from (https://www.continental-tires.com/car/tire-knowledge/tire-basics/tire-components).

- Davisson, J. A. Design and Application of Commercial Type Tires. *SAE Transactions, 78*, 1-32. (1969).
- Durairaj, R. B. *Resorcinol: Chemistry, Technology and Applications* (First edition ed.): Springer Berlin, Heidelberg, 2005.
- Frisch, K. C. Chapter 16 - Chemistry and technology of polyurethane adhesives11. In D. A. Dillard, A. V. Pocius, & M. Chaudhury (Eds.), *Adhesion Science and Engineering* (pp. 759-812). Amsterdam: Elsevier Science B.V, 2002.
- Gao, Y., Liu, J., Zhao, S., & Zhang, X. Qualitative Analysis of Tencel A100 Fiber and Selected Regenerated Cellulose Fibers. *AATCC Journal of Research, 4*(2), 10-14. (2017) Retrieved from (https://doi.org/10.14504/ajr.4.2.2).
- Gloriaful. Caprolactam Blocked Isocyanate MDI Crosslinker High Thermal Initiated PU-latent. (2022). Retrieved June 15, 2022 from (https://www.glorisochem.com/polyurethane-pu-crosslinker/blocked-isocyanate/caprolactam-blocked-isocyanate-mdi.html).
- Gupta, B. S. 1 - Manufacture, types and properties of biotextiles for medical applications. In M. W. King, B. S. Gupta, & R. Guidoin (Eds.), *Biotextiles as Medical Implants* (pp. 3-47): Woodhead Publishing, 2013.
- Information, N. C. f. B. PubChem Compound Summary for CID 7768, Caprolactam. (2022). Retrieved June 20, 2022 from (https://pubchem.ncbi.nlm.nih.gov/compound/Caprolactam).
- Ionescu, M. 2. Basic chemistry of polyurethanes. In (Vol. Volume 1, pp. 11-26): De Gruyter, 2019.
- Klempner, K. C. F. a. D. *Advances in Urethane Science and Technology* (1st ed. Vol. XIV). Boca Raton: Science & Technology, 1998.
- Lee, J. M., Subramani, S., Lee, Y. S., & Kim, J. H. Thermal decomposition behavior of blocked diisocyanates derived from mixture of blocking agents. *Macromolecular Research, 13*(5), 427-434. (2005). Retrieved from (https://doi.org/10.1007/BF03218476).
- Li, J., & Ma, E. Characterization of Water in Wood by Time-Domain Nuclear Magnetic Resonance Spectroscopy (TD-NMR): A Review. *Forests, 12*(7). (2021). Retrieved from (https://doi.org/10.3390/f12070886).
- Liessem, B. Foam manufacture. Kabel-und-Gummiwerke AG, Eupen, Belgium, 1983. Retrieved from (https://patents.google.com/patent/US4417002A/en).
- Lindenmuth, B. E. An overview of tire technology. *The pneumatic tire, 1*, 13136. (2006).
- Louis, A., Noordermeer, J. W., Dierkes, W. K., & Blume, A. *Technologies for Polymeric Cord/Rubber Adhesion in Tire Applications*. Paper presented at the 186th Technical Meeting of Rubber Division. Nashville, TN: *ACS*, 2014.
- Lugner, P. *Vehicle Dynamics of Modern Passenger Cars* (First ed.). Springer, Cham, 2019.
- Montgomery, D. C., & Runger, G. C. *Applied statistics and probability for engineers* (Third ed.). Arizona, United States of America: John Wiley & Sons Inc., 2003.
- Nakajima, Y. *Advanced Tire Mechanics* (First ed). Hachioji: Springer Nature, 2019.
- Neves, C. S. *Study of the dip content in tire textile reinforcements. TD-NMR as a method of analysis of the dip content*. Tese de Mestrado, Faculdade de Engenhariada da Universidade do Porto, Porto, Portugal, 2022.

- Nokian Tyres Plc. Reinforcing Materials in Rubber Products. U.S.A.: *Compound Development and Applications George Burrowes*, 2017.
- Pratapsi, M. D. S. *Study of Dip content in the tire textile reinforcement.* Tese de Mestrado, Faculdade de Engenhariada da Universidade do Porto, Porto, Portugal, 2017.
- Rocha, M. I. d. A. *Study of Dip content in the tire textile reinforcements.* Tese de Mestrado, Faculdade de Engenhariada da Universidade do Porto, Porto, Portugal, 2019.
- Rodrigues, K. A. O. *Adhesion promoters for tire textile reinforcements.* Tese de Mestrado, Universidade do Minho, Braga, Portugal, 2017.
- Rolph, M. S., Markowska, A. L. J., Warriner, C. N., & O'Reilly, R. K. (2016). Blocked isocyanates: from analytical and experimental considerations to non-polyurethane applications. *Polymer Chemistry, 7*(48), 7351-7364. Retrieved from (https://doi.org/10.1039/C6PY01776B).
- Santos, J. M. d. *Study of Dip content in the tire textile reinforcements.* Tese de Mestrado, Faculdade de Engenhariada da Universidade do Porto, Porto, Portugal, 2018.
- Silva, I. P. d. *Dip Content in the Tire Textile Reinforcements: A Comparation of Methods* Tese de mestrado, Faculdade de Engenhariada da Universidade do Porto, Porto, Portugal, 2020.
- Skedsoft. Tire Ply And Belted Design. (n.d.). Retrieved from (https://www.skedsoft.com/books/automobile-engineering/tire-ply-and-belt-design).
- Skeist, I. *Handbook of Adhesives* (Third edition ed.): Springer New York, NY, 1990.
- Subramanian, S., & Krishna, M. C. In Vivo Electron Paramagnetic Resonance Imaging. In *Reference Module in Chemistry, Molecular Sciences and Chemical Engineering*. Elsevier, 2014.
- Westgate, W., & Gillick, J. Key technology developments in textiles for use in automotive tires. *Textile Advances in the Automotive Industry, Woodhead Publishing, Cambridge, MA, USA*, 270-297. (2008).
- Xu, F., Dong, Y., Zhang, W., Zhang, S., Li, L., & Li, J. Preparation of cross-linked soy protein isolate-based environmentally-friendly films enhanced by PTGE and PAM. *Industrial Crops and Products, 67*, 373-380. (2015). Retrieved from (https://doi.org/10.1016/j.indcrop.2015.01.059).
- Zhang, H., Chen, K., Gao, X., Han, Q., & Peng, L. Improved thermal stability of regenerated cellulose films from corn (Zea mays) stalk pith using facile preparation with low-concentration zinc chloride dissolving. *Carbohydrate Polymers, 217*, 190-198. (2019). Retrieved from (https://doi.org/10.1016/j.carbpol.2018.10.107).

Annex A

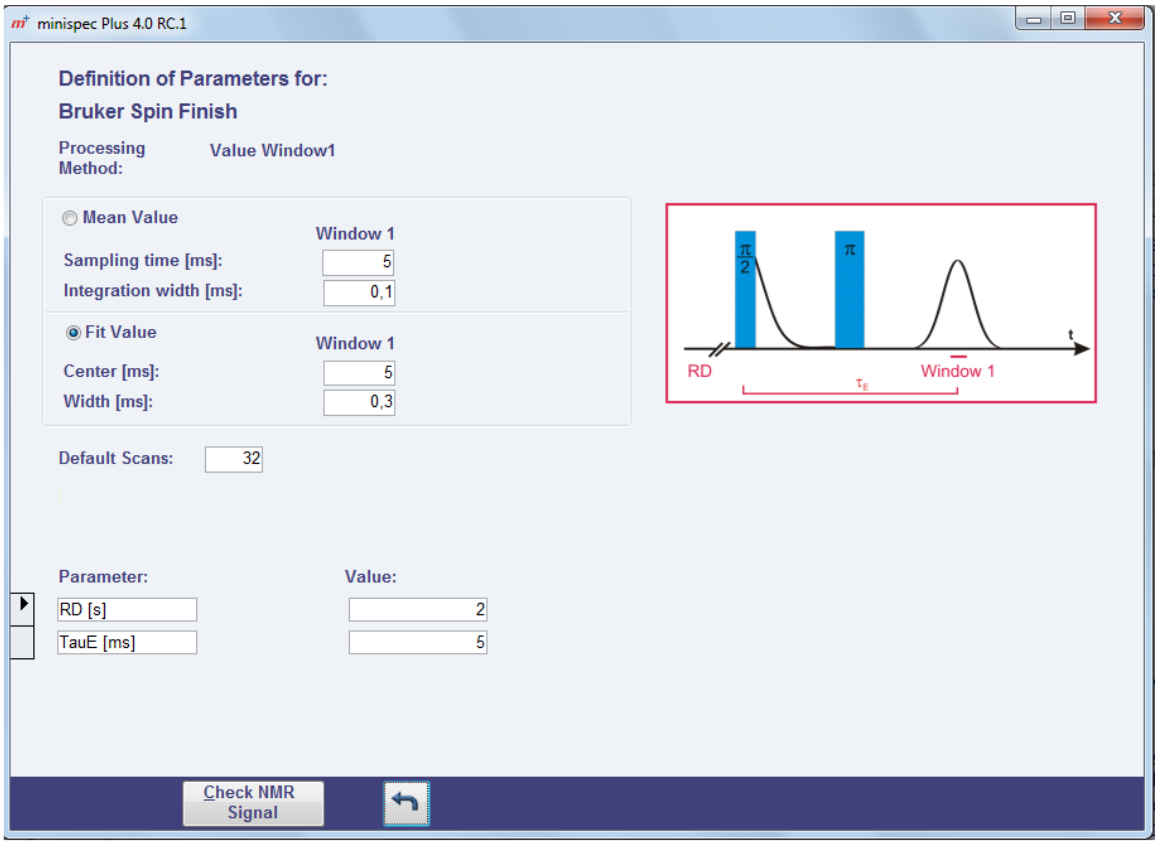

Figure A.1.Definition of parameters for Minispec Plus software.

Appendix A

A.1 Equation 6 deduction

Combining the Equations 3, 4 and 5 from 3.3.4 section,

$$\frac{m_{\text{dip}}}{\text{DPU}_{\text{per greige cord}}} \times 100 = \frac{m_{\text{dip}}}{\text{DPU}_{\text{per dipped cord}}} \times 100 - m_{\text{dip}} \tag{A.1}$$

Dividing both sides by m_{dip},

$$\frac{\frac{100}{\text{DPU}_{\text{per greige cord}}}}{m_{\text{dip}}} = \frac{\frac{m_{\text{dip}}}{\text{DPU}_{\text{per dipped cord}}}}{m_{\text{dip}}} \times 100 - 1 \tag{A.2}$$

resulting

$$\frac{100}{\text{DPU}_{\text{per greige cord}}} + 1 = \frac{100}{\text{DPU}_{\text{per dipped cord}}} \tag{A.3}$$

From Equation A.3, it is possible to make the conversion through the following equations

$$\text{DPU}_{\text{per dipped cord}} = \frac{100}{\frac{100}{\text{DPU}_{\text{per greige cord}}}+1} \tag{A.4}$$

$$\text{DPU}_{\text{per greige cord}} = \frac{\text{DPU}_{\text{per dipped cord}}}{100-\text{DPU}_{\text{per dipped cord}}} \times 100 \tag{A.5}$$

A.2 DPU standard methods

Table A.2.1. Influence of dissolution time on DPU_{WCM} values

Time / min	m_1 / g	m_2 / g	m_3 / g	DPU_{WCM} / %	Mean / %	SD / %	CV / %
30	1.0097	30.0493	30.0915	4.3618	4.48	0.12	2.60
	0.9994	29.9980	30.0419	4.5945			
	1.0457	26.7709	26.8158	4.4864			
40	1.0053	29.9944	30.0357	4.2842	4.16	0.11	2.61
	0.9898	26.9967	27.0357	4.0985			
	0.9992	26.8508	26.8901	4.0942			
60	1.0466	30.4120	30.4541	4.1911	4.14	0.05	1.12
	1.0287	29.9388	29.9793	4.0984			
	1.0027	29.9921	30.0320	4.1442			
75	1.0138	30.1997	30.2360	3.7136	3.84	0.06	1.62
	1.0964	30.3098	30.3499	3.7963			
	1.0078	30.0622	30.0999	3.8841			
90	1.0247	26.0707	26.1060	3.5678	3.60	0.05	1.50
	1.0094	30.3831	30.4178	3.5601			
	1.0005	30.4002	30.4355	3.6573			
120	1.0156	30.2813	30.3165	3.5904	3.63	0.03	0.90
	1.0638	30.2565	30.2940	3.6539			
	1.0033	26.2036	26.2388	3.6360			

Table A.2.2. DPU_{WCM} results for RFL and Cokoon dipped Rayon

Dipping solution	m_1 / g	m_2 / g	m_3 / g	DPU / %	Mean / %	SD / %	CV / %
RFL	1.0178	30.4115	30.4768	6.8556	6.79	0.08	1.15
	1.0180	26.6046	26.6695	6.8094			
	0.9997	26.0681	26.1309	6.7030			
RFL	1.0656	30.0288	30.1024	7.4194	7.14	0.01	0.16
	1.0078	30.4055	30.4726	7.1330			
	1.0476	30.3959	30.4658	7.1494			
RFL	0.9998	29.8943	29.9604	7.0794	7.14	0.08	1.13
	1.0003	30.3366	30.4029	7.0985			
	1.0444	26.3386	26.4090	7.2279			
Cokoon	1.0120	26.0579	26.0931	3.6036	3.61	0.03	0.93
	1.0002	26.2867	26.3219	3.6477			
	1.0296	26.5771	26.6127	3.5815			
Cokoon	1.0026	29.9934	30.0283	3.6065	3.67	0.07	1.86
	1.0040	26.6054	26.6416	3.7404			
	1.0189	30.4061	30.4420	3.6521			
Cokoon	1.0228	30.3722	30.4119	4.0382	3.61	0.01	0.41
	1.0737	30.2721	30.3094	3.5990			
	0.9933	30.4082	30.4429	3.6199			

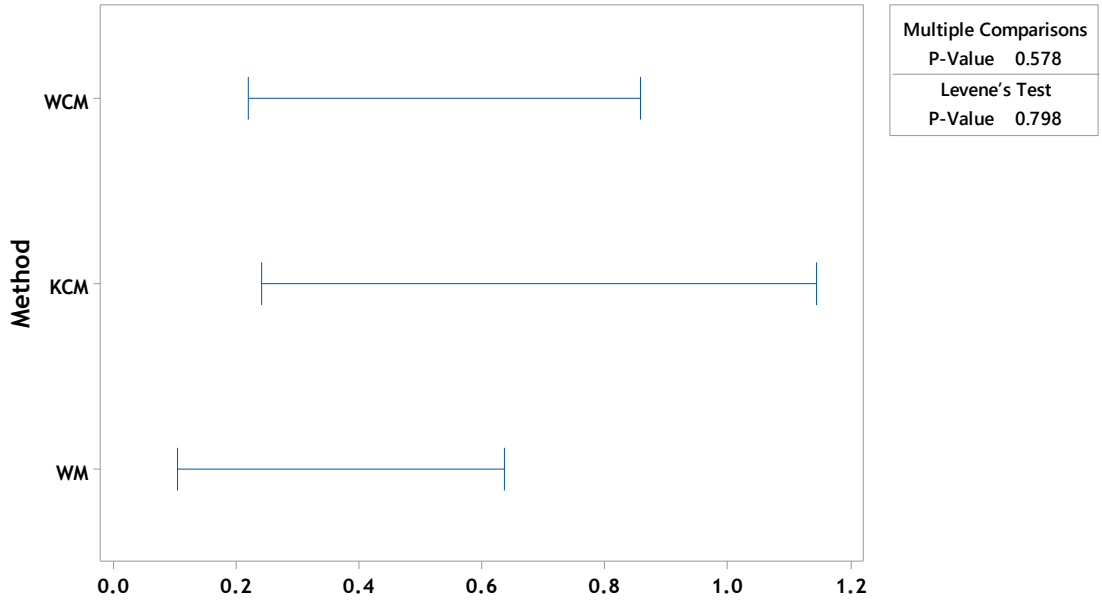

Figure A.2.1. Results from variance test for RFL dipping solution.

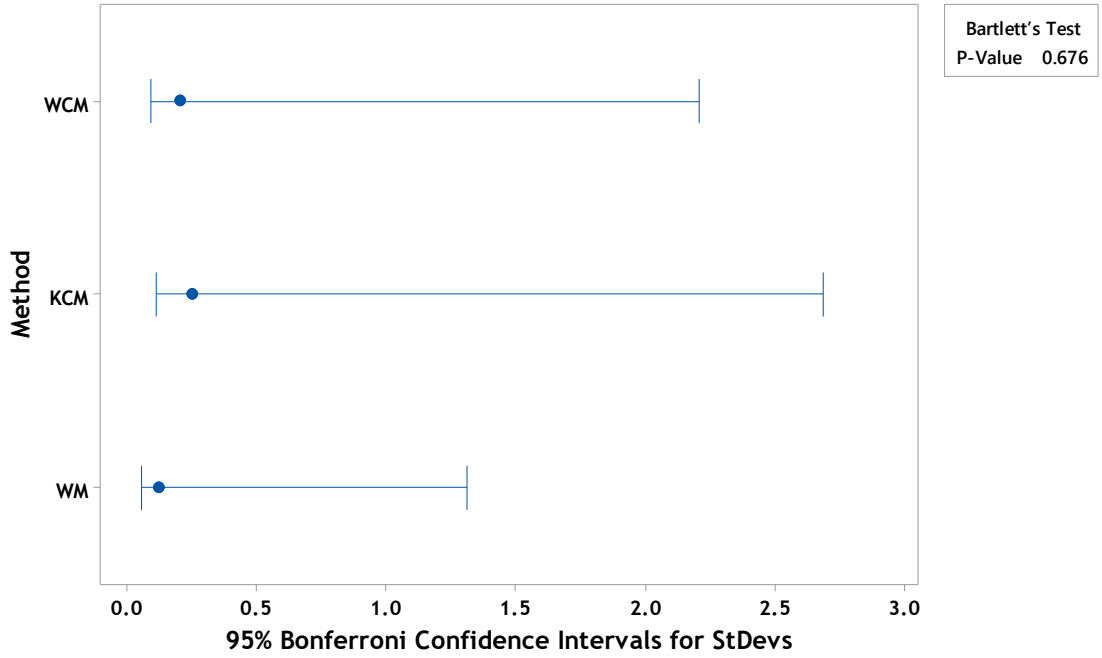

Figure A.2.2. Results from variance test for Cokoon dipping solution.

Table A.2.3. One-way ANOVA results: DPU versus RFL dipping solution

	Mean / %	95 % CI	SE / %	p-value
WCM	7.023	(6.746, 7.301)		
KCM	8.077	(7.799, 8.354)	0.196	1.586×10^{-3}
WM	7.340	(7.063, 7.6174)		

Table A.2.4. One-way ANOVA results: DPU versus Cokoon dipping solution

	Mean / %	**95 % CI**	**SE / %**	**p-value**
WCM	3.630	(3.498, 3.762)		
KCM	4.530	(4.398, 4.662)	0.093	1.392×10^{-6}
WM	5.393	(5.261, 5.526)		

A.3 TD-NMR

Table A.3.1. $DPU_{per\ greige\ cord}$ *measurements with WCM for Cokoon dipped Rayon samples necessary to perform the TD-NMR calibration*

Cords	m_1 / g	m_2 / g	m_3 / g	DPU / %	Mean / %	SD / %
A	1.0409	30.0569	30.0745	1.7199	1.56	0.03
	1.0419	30.2806	30.2968	1.5794		
	1.0133	30.3953	30.4107	1.5432		
B	1.0706	30.1388	30.1722	3.2202	3.21	0.08
	1.0332	30.2729	30.3042	3.1241		
	1.0985	29.9392	29.9741	3.2813		
C	1.0962	30.3092	30.3599	4.8494	4.85	0.04
	0.9938	30.4081	30.4545	4.8976		
	1.0259	30.3719	30.4190	4.8120		
D	0.9913	30.0315	30.0838	5.5698	5.62	0.05
	0.9918	30.1388	30.1920	5.6680		
	1.0027	29.9388	29.9921	5.6141		

Table A.3.2. $DPU_{per\ greige\ cord}$ *measurements with WM for Cokoon dipped Rayon samples necessary to perform the TD-NMR calibration*

Cords	$m_{Greige\ cord}$ / g	$m_{Dipped\ cord}$ / g	DPU / %	Mean / %	SD / %	CV / %
A	3.8044	3.9185	2.9992	2.95	0.05	1.76
	3.8044	3.9165	2.9466			
	3.8044	3.9187	3.0044			
	3.8044	3.9140	2.8809			
	3.8044	3.9143	2.8888			
	3.8044	3.9170	2.9597			
	3.8044	3.9185	2.9992			
	3.8044	3.9142	2.8861			
	3.8044	3.9189	3.0097			
	3.8044	3.9174	2.9702			
B	3.8044	4.0167	5.5804	5.51	0.09	1.60
	3.8044	4.0155	5.5488			
	3.8044	4.0113	5.4384			
	3.8044	4.0091	5.3806			
	3.8044	4.0131	5.4858			
	3.8044	4.0190	5.6408			
	3.8044	4.0180	5.6146			
	3.8044	4.0154	5.5462			
	3.8044	4.0110	5.4306			
	3.8044	4.0113	5.4384			
C	3.8044	4.0727	7.0524	7.09	0.12	1.73
	3.8044	4.0677	6.9209			
	3.8044	4.0741	7.0892			
	3.8044	4.0735	7.0734			
	3.8044	4.0800	7.2442			
	3.8044	4.0775	7.1785			
	3.8044	4.0759	7.1365			
	3.8044	4.0738	7.0813			
	3.8044	4.0656	6.8657			
	3.8044	4.0797	7.2364			
D	3.8044	4.0953	7.6464	7.78	0.16	2.02
	3.8044	4.0979	7.7148			
	3.8044	4.0937	7.6044			
	3.8044	4.1040	7.8751			
	3.8044	4.1015	7.8094			
	3.8044	4.1005	7.7831			
	3.8044	4.1137	8.1301			
	3.8044	4.1001	7.7726			
	3.8044	4.0935	7.5991			
	3.8044	4.1028	7.8435			

Table A.3.3. DPU reference values, mass of the dried sample and Td-NMR results (signal) for the WCM_{curve}

Sample	DPU per greige cord / %	DPU per dipped cord / %	$m_{(tube+lid)}$ / g	$m_{(tube+lid+dried\ sample)}$ / g	$m_{(dried\ sample)}$ / g	Signal
A	1.56	1.69	16.1938	16.5831	0.3893	41.45
		1.55	16.1632	16.6412	0.4780	41.82
		1.52	16.2152	16.6080	0.3928	42.32
B	3.21	3.12	16.2639	16.6599	0.3960	89.84
		3.03	16.3638	16.7850	0.4212	91.03
		3.18	16.2293	16.6410	0.4117	89.30
C	4.85	4.63	16.2070	16.4840	0.2770	128.87
		4.67	16.2668	16.6290	0.3622	124.91
		4.59	16.3193	16.6525	0.3332	130.96
D	5.62	5.28	16.2297	16.5410	0.3113	143.02
		5.36	16.2506	16.5770	0.3264	146.86
		5.32	16.3432	16.5090	0.1658	141.11

Table A.3.4. DPU reference values, mass of the dried sample and Td-NMR results (signal) for the WM_{curve}

Sample	DPU per greige cord / %	DPU per dipped cord / %	$m_{(tube+lid)}$ / g	$m_{(tube+lid+dried\ sample)}$ / g	$m_{(dried\ sample)}$ / g	Signal
A	2.95	2.87	16.1938	16.5831	0.3893	40.32
		2.87	16.1632	16.6412	0.4780	41.59
		2.87	16.2152	16.6080	0.3928	41.17
B	5.51	5.22	16.2639	16.6599	0.3960	89.45
		5.22	16.3638	16.7850	0.4212	89.18
		5.22	16.2293	16.6410	0.4117	90.20
C	7.09	6.62	16.2070	16.4840	0.2770	125.91
		6.62	16.2668	16.6290	0.3622	126.17
		6.62	16.3193	16.6525	0.3332	129.44
D	7.78	7.22	16.2297	16.5410	0.3113	146.82
		7.22	16.2506	16.5770	0.3264	148.70
		7.22	16.3432	16.5090	0.1658	139.07

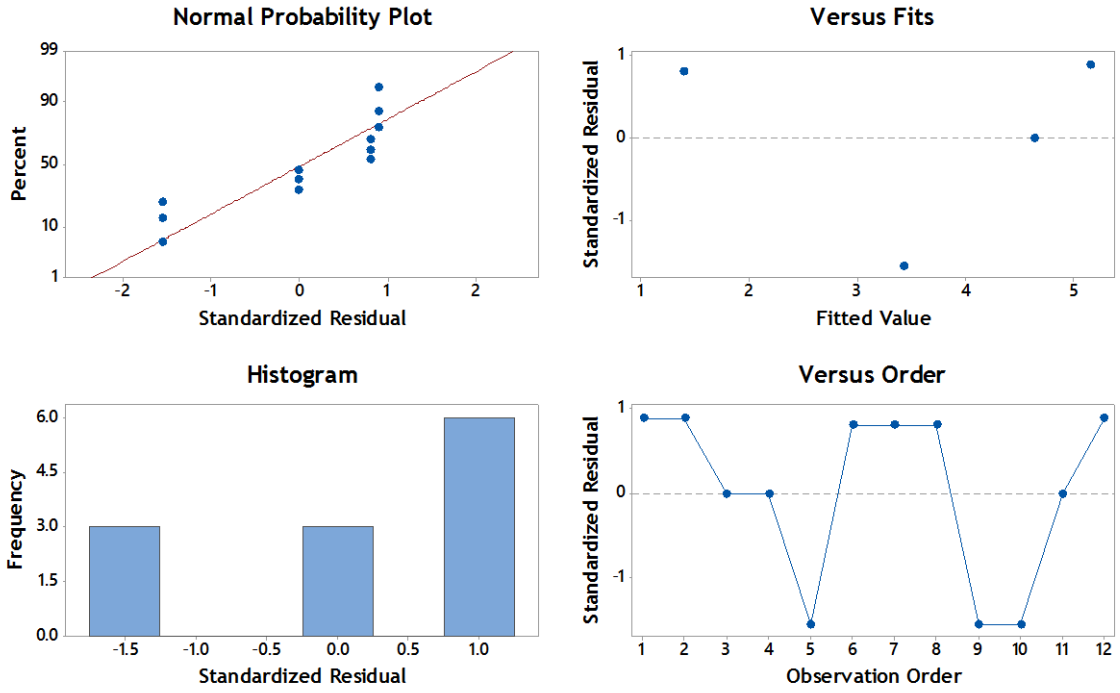

Figure A.3.1. Residual plots for correlation corresponded to the regression DPU_{WM} vs DPU_{WCM}.

Table A.3.5. DPU_{WCM} results for twenty samples collected by the Production Department

	m_1 / g	m_2 / g	m_3 / g	DPU / %	Mean / %	SD / %
P1	0.9998	26.3248	26.3589	3.5311	3.52	0.16
	1.0032	29.9400	29.9756	3.6792		
	1.0078	30.2725	30.3052	3.3535		
P2	1.0607	26.2439	26.2778	3.3015	3.25	0.09
	1.0599	29.9379	29.9718	3.3041		
	0.9972	30.3091	30.3396	3.1551		
P3	1.0241	30.0601	30.0939	3.4131	3.26	0.23
	1.1160	30.0304	30.0668	3.3716		
	0.9961	30.2726	30.3016	2.9987		
P4	1.0045	26.5806	26.6087	2.8779	3.19	0.27
	1.0684	30.1345	30.1687	3.3069		
	1.0132	30.2813	30.3144	3.3772		
P5	1.0029	30.3730	30.4033	3.1154	3.05	0.10
	1.0143	26.0495	26.0800	3.1002		
	1.0031	30.4071	30.4357	2.9348		
P6	0.9967	30.3070	30.3462	4.0940	3.74	0.46
	1.0096	26.2421	26.2800	3.9004		
	1.0529	30.0621	30.0950	3.2255		
P7	1.0055	30.1383	30.1727	3.5424	3.45	0.18
	1.0165	30.2833	30.3152	3.2399		
	1.0227	29.9349	29.9700	3.5541		
P8	1.0283	30.3067	30.3420	3.5549	3.56	0.25

	1.0035	26.2409	26.2778	3.8175		
	1.0050	26.5787	26.6109	3.3100		
	1.0130	26.2064	26.2386	3.2830		
P9	1.0180	30.0307	30.0611	3.0782	3.11	0.16
	1.0199	30.3748	30.4041	2.9578		
	1.0232	29.9382	29.9734	3.5628		
P10	1.0492	30.1377	30.1721	3.3898	3.61	0.25
	1.0880	30.3083	30.3489	3.8763		
	1.0508	30.0607	30.0964	3.5169		
P11	1.0844	30.4066	30.4426	3.4338	3.43	0.09
	1.0198	30.2696	30.3025	3.3337		
	1.0337	30.4025	30.4364	3.3907		
P12	1.0661	30.2699	30.3055	3.4546	3.38	0.08
	1.0523	30.0604	30.0940	3.2983		
	1.0015	30.0299	30.0610	3.2049		
P13	1.0753	30.3735	30.4120	3.7133	3.42	0.26
	1.1532	30.3073	30.3447	3.3519		
	1.0407	30.1369	30.1694	3.2236		
P14	1.0816	29.9378	29.9735	3.4133	3.30	0.10
	1.0228	30.4074	30.4397	3.2610		
	1.0224	30.4039	30.4403	3.6917		
P15	1.0104	29.9363	29.9744	3.9185	3.73	0.17
	1.0019	30.1374	30.1721	3.5877		
	1.0408	26.2398	26.2719	3.1823		
P16	1.0549	30.3923	30.4288	3.5841	3.39	0.20
	1.0053	26.5815	26.6145	3.3940		
	1.0082	30.3933	30.4271	3.4688		
P17	1.0222	30.3087	30.3419	3.3569	3.51	0.18
	1.0314	29.9378	29.9747	3.7104		
	1.1259	30.0597	30.0965	3.3789		
P18	1.0008	30.2813	30.3152	3.5061	3.42	0.07
	1.0265	26.2040	26.2375	3.3736		
	1.0218	30.0635	30.0934	3.0144		
P19	1.0304	30.2836	30.3156	3.2051	3.12	0.10
	1.0741	30.4064	30.4390	3.1301		
	1.0384	30.1400	30.1741	3.3954		
P20	1.0019	30.0339	30.0672	3.4380	3.40	0.04
	1.0234	30.3734	30.4066	3.3529		

Table A.3.6. Comparation between the DPU results obtained by the TD-NMR and Weighing Method (correlation) for the twenty samples collected

Sample	Date	TD-NMR		Wet-Chemical		Weighing	
		DPU_{per} total cord / %	DPU_{per} greige cord / %	DPU_{per} greige cord / %	DPU_{per} dipped cord / %	DPU_{per} dipped cord / %	DPU_{per} greige cord / %
1	12/03/2020	3.97	4.13	3.52	3.40	5.19	5.48
2	12/03/2020	4.28	4.47	3.25	3.15	4.90	5.16
3	28/03/2020	3.85	4.00	3.26	3.16	4.91	5.17
4	19/04/2020	4.04	4.21	3.19	3.09	4.83	5.08
5	19/04/2020	3.88	4.04	3.05	2.96	4.68	4.91
6	12/05/2020	4.40	4.60	3.74	3.61	5.43	5.74
7	03/07/2020	4.01	4.17	3.45	3.33	5.11	5.39
8	03/07/2020	4.08	4.25	3.56	3.44	5.24	5.53
9	27/07/2020	3.30	3.41	3.11	3.01	4.74	4.98
10	13/09/2020	4.48	4.69	3.61	3.48	5.29	5.59
11	21/12/2020	3.91	4.07	3.43	3.31	5.09	5.37
12	01/02/2021	4.35	4.54	3.38	3.27	5.04	5.31
13	01/02/2021	3.94	4.10	3.42	3.31	5.09	5.36
14	01/02/2021	4.30	4.49	3.30	3.19	4.95	5.21
15	13/01/2021	4.80	5.04	3.73	3.60	5.42	5.73
16	17/02/2021	4.61	4.83	3.39	3.28	5.05	5.32
17	17/02/2021	4.57	4.79	3.51	3.39	5.18	5.47
18	17/02/2021	4.63	4.86	3.42	3.31	5.08	5.36
19	08/01/2022	5.03	5.30	3.12	3.02	4.76	4.99
20	15/02/2022	5.38	5.69	3.40	3.28	5.06	5.33

Table A.3.7. Variance test results for the population of Cokoon dipped Rayon

	SD / %	Variance	95 % CI for σ	Estimated ratio of SD	95 % CI for Ratio using Bonnett	95 % CI for Ratio using Levene
TD-NMR	0.518	0.269	(0.368, 0.809)	2.228	(1.251, 3.547)	(1.308,3.915)
WM	0.233	0.054	(0.180, 0.334)			

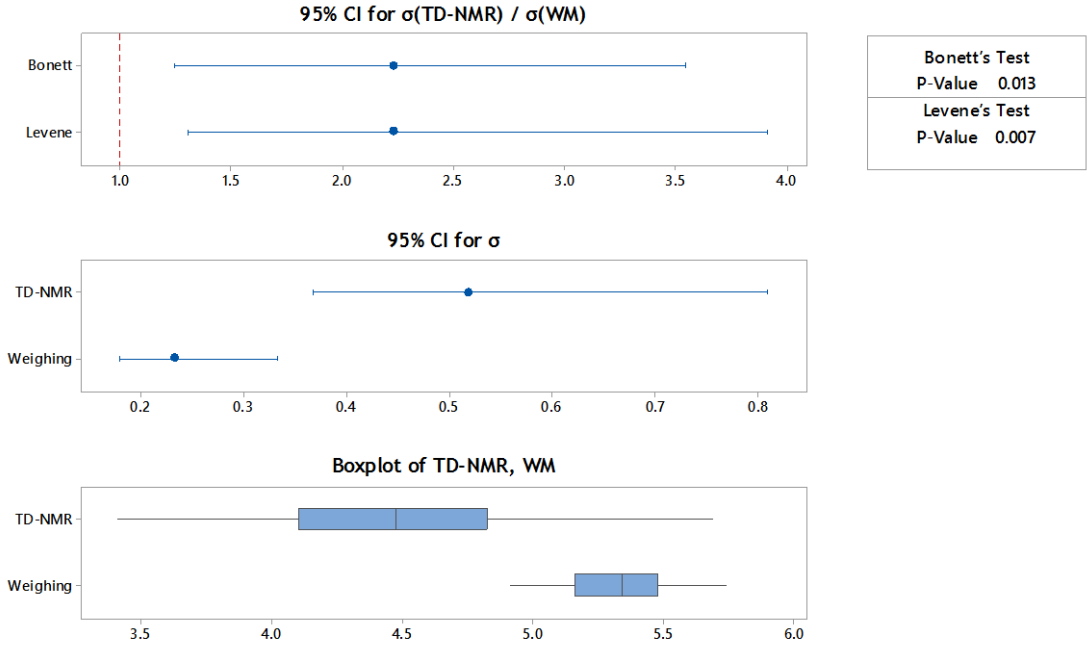

Figure A.3.2. Test and 95 % CI for Two Variances: TD-NMR and WM.

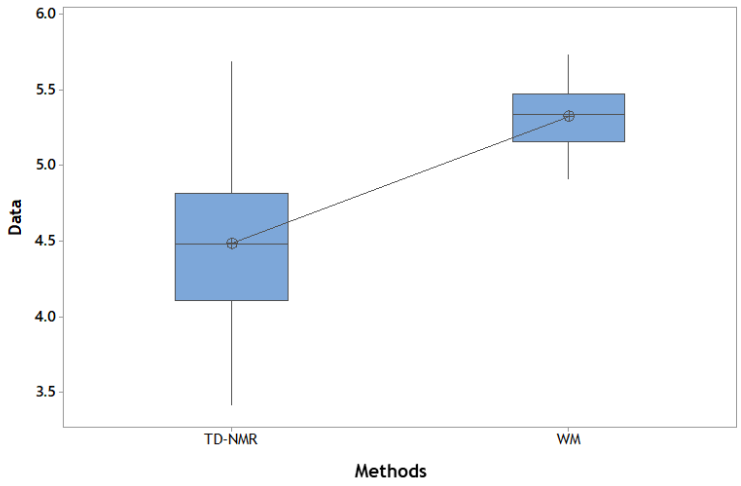

Figure A.3.3. Boxplot representation of the DPU values with the samples mean for both methods: TD-NMR and Weighing.